Food & Function

ROYAL SOCIETY OF CHEMISTRY

PAPER

View Article Online
View Journal | View Issue

Cite this: *Food Funct.*, 2025, **16**, 943

Protective effect of a combination of multiple strains of *Lactobacillus acidophilus* on collagen-induced arthritis†

Yang Yang, [a,b] Qing Hong,[a,b] Xuehong Zhang[c] and Zhenmin Liu *[a,b]

Rheumatoid arthritis (RA) is a systemic, chronic autoimmune disease. Many studies have shown that microorganisms may be an important pathological factor leading to the onset of RA. Some infectious or non-infectious pathogenic microorganisms and their metabolites may be the initiating factors of the early onset of RA. The aim of this study was to alleviate RA by regulating the imbalance of the gut microbiota in the early stage of RA using mixed bacterial strains. The mixed strains of *Lactobacillus acidophilus* (BD18, NCFM, BD1802, BD3545, BD5032) significantly reduced the clinical score and swelling thickness of the paws of collagen-induced arthritis (CIA) rats. The expression of TNF-α and MMP-13 proteins in the joints of CIA rats was also inhibited. The levels of specific antibodies (anti-CII IgG, anti-CII IgG1, anti-CII IgG2a, and anti-CII IgG2b) and inflammatory factor IL-6 in the serum of CIA rats were also significantly reduced. The relative abundance of *Lactobacillus*, *Clostridia*_UCG-014, *Ruminococcus*, *Candidatus*_*Saccharimonas*, *Romboutsia*, *Turicibacter*, and *Clostridium*_*sensu*_*stricto*_1 in the gut microbiota of CIA rats receiving oral administration of the mixed strains of *L. acidophilus* was significantly reduced, bringing their microbiota closer to that of healthy rats. Moreover, the levels of intestinal metabolites of short chain fatty acids in CIA rats, acetic acid and butyric acid, were significantly increased. The mixed strains of *L. acidophilus* could recover the relative abundance of *Ligilactobacillus*, *Clostridia*_UCG-014_unclassified, *Ruminococcus*, *Candidatus*_*Saccharimonas*, *Romboutsia* and *Turicibacter*, affecting purine metabolism, transcription factors and alanine metabolism, and reducing the levels of specific antibodies and inflammatory factors in the blood, finally slowing the development of experimental arthritis induced by CII, which exerts the protective effect of probiotics. Mixed *L. acidophilus* strains are more effective than a single strain, and the effect is not the result of a single strain, but of a combination of strains.

Received 29th October 2024,
Accepted 26th December 2024

DOI: 10.1039/d4fo05273k

rsc.li/food-function

1. Introduction

Rheumatoid arthritis (RA) is a chronic autoimmune disease that manifests as bone erosion, synovitis and joint destruction, even permanent disabilities. The disease is marked by polyarticular inflammation involving multiple immune cells, inflammatory cytokines, and autoantibodies. The prevalence of RA is in approximately 1% of the global population,[1] with about 75% of affected individuals being women.[2] Various genetic and environmental factors contribute to the onset of RA. Many genes are related to RA susceptibility risk, such as high-risk HLA-DR alleles, BACH2, and CDK5RAP2.[3] Environmental factors, such as smoking, microorganisms, and diet, also play a significant role in the disease's development.[4] Epidemiological and translational studies have demonstrated a strong connection between mucosal environmental exposures and/or dysbiosis of intestinal flora and the onset of RA,[5–7] supporting the "mucosal origin hypothesis". This hypothesis posits that RA development begins at one or more sites in the mucosa.

The pathogenesis of RA is extremely complex and unclear. Multiple studies have shown that most patients will have experienced a long period of serological RA-related autoantibody positivity before the first clinical symptoms of RA.[8–12] During the long period, a variety of serum autoantibodies are generated, including two primary types: anti-citrullinated protein antibodies (ACPAs) and rheumatoid factors (RFs) that recognize the Fc domain. Notably, ACPAs and RFs are produced in the local mucosa of 40% individuals who have familial or clinical risk factors but have not yet developed arthritis.[13] However, local

[a]*State Key Laboratory of Dairy Biotechnology, Shanghai Engineering Research Center of Dairy Biotechnology, Shanghai, China. E-mail: liuzhenmin@brightdairy.com*
[b]*Dairy Research Institute, Bright Dairy & Food Co., Ltd, Shanghai, China*
[c]*State Key Laboratory of Microbial Metabolism, and School of Life Sciences and Biotechnology, Shanghai Jiao Tong University, Shanghai, China*

† Electronic supplementary information (ESI) available. See DOI: https://doi.org/10.1039/d4fo05273k

autoantibodies originate in one of many sites that could vary with each patient. Molecular mimicry has been suggested as a possible cause of several autoimmune diseases.[14–16] Molecular mimicry provides a bridge between symbiotic microbiomes with genetic risk. The host immune system identifies $CD4^+$ T cells that respond to symbiotic microbial and self-antigens that share similar motifs, which contributes to the development of classified RA. With these observations and the knowledge gained from these studies, the susceptibility genes plus the mishandling symbiotic microbes of the immune system make individuals vulnerable to RA. Even if the host symbiotic microorganism cannot be completely eliminated, is it possible to regulate it to alleviate disease? Disease progression is influenced by the supplementation of probiotics to regulate the abundance of gut bacteria that produce antigen-mimics. A study implied that *Lacticaseibacillus casei* CCFM1074 intervention alleviated collagen-induced arthritis (CIA) in rats by modulating the metabolites and gut microbiota.[17] This study seeks to search an approach for restoring the immune balance by supplementing probiotics rather than eliminating the factors causing immune imbalance.

Probiotics are often used to regulate host gut microbiota and restore intestinal balance. Probiotics suppress pathogens by interacting with host microbiota and contribute to the suppression of inflammatory cytokines.[18,19] The CIA model is widely applied in the study of RA because CIA has many similarities with human RA. Two features of the CIA model – the destruction of immune tolerance and the production of autoantibodies – make the CIA the gold standard *in vivo* model for RA research. In addition, the presence of dysbiosis was observed in the model. As RA progresses, the abundance of the families *Bacteroidaceae*, *Lachnospiraceae*, and S24-7 significantly increases in CIA-susceptible mice. Fecal microbiota from CIA-susceptible mice were transferred to germ-free mice, and the germ-free mice showed susceptibility to arthritis.[20] This study aims to investigate whether early intervention with probiotics can alleviate RA.

In our study, we selected several groups of mixed strains of probiotics, including *Lacticaseibacillus casei* (ATCC393, BD386, BD418, BD3535, BD389), *Limosilactobacillus reuteri* (BD76, BD2766, BD2790, BD5277, BD5294), *Bifidobacterium* (BD3150, BD400, BD5348, BD6256, BB12), and *Lactobacillus acidophilus* (BD18, NCFM, BD1802, BD3545, BD5032), to screen for probiotics with protective effects against RA. We evaluated the weight of the rats, the clinical scores of arthritis in the paws, and the swelling thickness of the paws to compare the effects of probiotics on the onset and progression of arthritis symptoms in CIA rats. Histological assessments, including haematoxylin and eosin staining, safranin O-fast green staining, and immunofluorescence staining, were employed to determine knee joint tissue damage and the expression of pro-inflammatory factors in CIA rats. The production of specific antibodies and cytokines in the serum of CIA rats was quantified using an ELISA kit. Additionally, 16S rDNA sequencing technology and gas chromatography-mass spectrometry (GC-MS) were utilized to analyze changes in the gut microbiota and the production of short-chain fatty acids in rat stool. In this study, the screened mixed strains of probiotics were further isolated into single strains for comparative analysis to explore whether the combination of multiple strains or a single strain plays a role in protection against RA.

2. Materials and methods

2.1. Materials and reagents

Bovine type II collagen solution, complete Freund's adjuvant and incomplete Freund's adjuvant were purchased from Chondrex (Redmon, WA, USA). Methotrexate (MTX) and dexamethasone (DXMS) was purchased from Shanghai Yuanye Bio-Technology Co. Ltd (Shanghai, China). The anti-TNF-α antibody and anti-MMP-13 antibody were purchased from Abcam (Cambridge, United Kingdom). The total CII-IgG ELISA kit, CII-IgG1 ELISA kit, CII-IgG2a ELISA kit and CII-IgG2b ELISA kit were purchased from Shanghai MuLuan Biological Technology Co. Ltd (Shanghai, China). The rat TNF-α ELISA kit, rat IL-1β ELISA kit and rat IL-17A ELISA kit were purchased from Hangzhou Lianke Biotechnology Co. Ltd (Hangzhou, China).

2.2. Bacterial strains

All the *Lactobacillus* species were cultured in de Man–Rogosa–Sharpe (MRS) broth and cultivated overnight at 37 °C. All the *Bifidobacterium* species were cultured in MRS broth with 0.5% L-cysteine at 37 °C overnight. Bacterial cells were harvested by centrifugation at 3000*g* for 10 min at 4 °C. The bacterial precipitate was washed twice with sterile saline. All the bacterial cells were re-suspended in sterile 30% (w/w) sucrose and colonies were counted. These bacterial solutions were stored at −80 °C prior to use. Before daily oral administration, the concentration of each strain was re-suspended at 2×10^8 CFU mL^{-1} in sterile saline. According to Table 1, five strains were mixed into a bacterial solution for daily oral administration.

Table 1 Probiotics used in this study

Group	Strains
L. casei	*L. casei* ATCC 393
	L.casei BD386 (LC2W)
	L. casei BD418
	L. casei BD3535 (L15)
	L. casei BD389 (BDII)
L. reuteri	*L. reuteri* BD76
	L. reuteri BD2766
	L. reuteri BD2790
	L. Reuteri BD5277
	L. reuteri BD5294
Bifidobacterium	*B. longum* BD3150
	B. animalis BD400
	B. longum BD6256 (PP4)
	B. bifidum BD5348
	B. breve BB12
L. acidophilus	*L. acidophilus* BD18
	L. acidophilus BD399 (NCFM)
	L. acidophilus BD1802
	L. acidophilus BD3545
	L. acidophilus BD5032

All the probiotics used in this study were from the bacteria bank at the State Key Laboratory of Dairy Biotechnology and are listed in Table 1.

2.3. Experimental animals

Female Wistar rats, 7–8 weeks of age, were purchased from Shanghai SLAC Laboratory Animal Ltd (Shanghai, China). The Wistar rats were housed under specific pathogen-free conditions at 25 ± 2 °C and humidity of 50% ± 5%, with a 12 h light–dark cycle. Food and water were given *ad libitum*. Rats were acclimatized for 7 days before the experiment was initiated. All animal experiments were conducted in compliance with the Regulations for the Administration of Affairs Concerning Experimental Animals in China. The protocols for this study received approval from the Institutional Animal Care and Use Committee of Shanghai Rat & Mouse Biotech Co. Ltd (Approval No. 202211(17)).

2.4. Induction of CIA rat model and treatment

The CIA rat model was established referring to a previous method.[21] Briefly, 2 mg mL^{-1} bovine type II collagen (CII) was dissolved in 0.05 M acetic acid and then emulsified in an equal volume of complete Freund's adjuvant. For primary immunization, Wistar rats were induced by subcutaneous injection with 0.15 mL of emulsion at the base of the tail. After 7 days, the rats received a booster immunization with the same volume of CII emulsified in incomplete Freund's adjuvant.

Wistar rats were randomly divided into seven groups (eight rats per each group), including the control group, CIA group, positive drug group, *Lacticaseibacillus casei* group, *Limosilactobacillus reuteri* group, *Bifidobacterium* group, and *Lactobacillus acidophilus* group. Rats in the control and CIA groups were orally administered with 1.5 mL of sterile normal saline. Rats in the positive drug group received intragastric administration of 1.5 mL of sterile normal saline daily for two weeks. After the primary immunization, methotrexate (7.6 mg per kg bw per week) was used as the standard drug twice a week in the positive drug group. Rats in the bacterial solution group (*Lacticaseibacillus casei* group, *Limosilactobacillus reuteri* group, *Bifidobacterium* group, and *Lactobacillus acidophilus* group) were orally administered with 1.5 mL of bacterial solution (2×10^8 CFU mL^{-1}) daily. The experiment schedule is shown in Fig. 1.

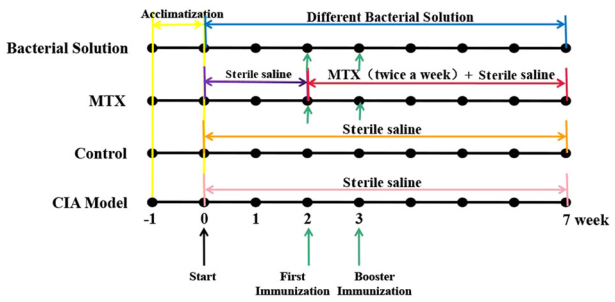

Fig. 1 Experiment schedule.

2.5. Assessment of CIA

Collagen-induced arthritis was assessed by the thickness of the hind paw, arthritis score and body weight. The thickness of the hind paw was measured using a caliper once a week after the primary immunization. After the primary immunization, the severity of arthritis was scored for each foot weekly according to the following ordinal scale:[21] 0, no swelling or erythema; 1, slight swelling and/or erythema; 2, marked swelling and/or erythema; 3, severe swelling and deformity; and 4, maximal swelling and deformity with ankylosis. The total score for each rat was calculated as an arthritis score with a maximum value of 16. The body weight and the paw thickness of the CIA rats were measured weekly from the beginning of the experiment.

2.6. Histopathological analysis

After sacrifice, rat knee joints were harvested and fixed in 4% paraformaldehyde. The joints were decalcified with 10% EDTA for 30 days, embedded in paraffin, and then sliced into 5 μm thick sections. The sections were stained using haematoxylin and eosin (H&E) and safranin O-fast green staining for histopathological analysis.

2.7. Immunofluorescence staining

After fixation in formalin, joints were embedded in paraffin and sectioned into 5-μm slices. Following deparaffinization and antigen retrieval, the sections were incubated overnight at 4 °C with the primary antibodies anti-TNF-α and anti-MMP-13, respectively. After washing, the sections were incubated for 1 h at room temperature in the dark with secondary goat anti-rabbit IgG antibodies. Subsequent washing was performed, and 4′,6-diamidino-2-phenylindole (DAPI) was applied for cell nuclei staining at room temperature for 5 min in the dark. The samples were then sealed and examined under a fluorescence microscope.

2.8. Determination of collagen-specific IgG and inflammatory factors

After anesthetizing rats with isoflurane, cardiac blood was collected. After keeping at room temperature for 30 min, serum was harvested by centrifugation at 3000*g* for 20 min at room temperature. The serum was stored at −80 °C until analysis. Total II collagen-specific IgG (CII-IgG), and its subclasses CII-IgG1, CII-IgG2a and CII-IgG2b were determined using ELISA kits according to the manufacturer's instructions. The levels of interleukin-1β (IL-1β) and interleukin-6 (IL-6) in the serum were measured using ELISA kits according to the manufacturer's instructions.

2.9. Quantitative real-time PCR

The intestinal permeability-related genes in the ileum of rats were assayed. RNA was extracted from ileal tissues using TRIzol reagent (Invitrogen Life Technologies, Carlsbad, CA) following the manufacturer's instructions. Quantitative real-time PCR (qPCR) was conducted using iTaq Master SYBR

Table 2 Primers used in quantitative real-time PCR

Genes	Primer sequence (5′-3′)
ZO-1	F: 5′-TTTTTGACAGGGGGAGTGG-3′ R: 5′-TGCTGCAGAGGTCAAAGTTCAAG-3′
Occludin-1	F: 5′-GTCTTGGGAGCCTTGACATCTT-3′ R: 5′-GCATTGTCGAACGTGCATC-3′
Claudin-1	F: 5′-GGGACAACATCGTGACTGCT-3′ R: 5′-CCACTAATGTCGCCAGACCTG-3′
MUC-2	F: 5′-AGATCCCGAAACCATGTC-3′ R: 5′-GTTCCACATGAGGGAGAGG-3′
β-Actin	F: 5′-TCAGGTCATCACTATCGGCAAT-3′ R: 5′-AAAGAAAGGGTGTAAAACGCA-3′

Green SuperMix (Bio-Rad, Hercules, CA) in an RT PCR system (Thermal Cycler CFX96, Bio-Rad, Hercules, CA). The relative expression of genes was normalized to that of β-actin and calculated using the $2^{-\Delta\Delta CT}$ method. Primers used are shown in Table 2.

2.10. Sequencing of the gut microbiota in feces

Fecal samples were collected at the end of the experiment and stored at −80 °C prior to use. Total DNA was extracted from fecal samples using the FastDNA Spin Kit (Tiangen Biotech, Beijing, China) following the manufacturer's instructions. The V3–V4 region of 16S rDNA was amplified using 341/806 primer pairs. Phusion High-Fidelity PCR Master Mix (New England Biolabs, Ipswich, MA, UK) was employed for PCR amplification. The amplified products were purified through 1% agarose gel using a gel extraction kit (Tiangen, Beijing, China). The purified samples were quantified using Qubit 2.0 (Life Technologies, CA, USA) and adjusted to equimolar solution, pooled and library prepared, followed by sequencing in the Illumina MiSeq platform as per the manufacturer's instructions.

Sequenced raw data were analyzed using the QIIME2 pipeline with DADA2. The representative sequences were classified according to the Silva 16S reference database with a 97% threshold. The biodiversity of the gut microbiota was predicted using PICRUSt. Alpha diversity was assessed by Chao1, Simpson and Shannon indexes. Beta diversity was evaluated using the Bray–Curtis distances and unweighted UniFrac distances, which were visualized through principal component analysis (PCA), principal coordinate analysis (PCoA), non-metric multidimensional scaling (NMDS) and analysis of similarities (Anosim). Linear discriminant analysis Effect Size (LEfSe) analysis was conducted to identify discriminatory taxa among groups, with LDA values greater than 3.0 and *p*-values less than 0.05 considered significant. Spearman's correlation analysis was performed to evaluate the potentially relevant associations on the gut microbiota of rats.

2.11. Determination of SCFAs in feces

Fecal samples and water were mixed in a vortex at a ratio of 2 : 1 for 10 s. Steel balls were added to the sample, treated with a 40 Hz grinder for 4 min, and then subjected to ultrasound treatment for 5 min (ice water bath); this was repeated 3 times. The samples were centrifuged at 5000 rpm for 20 min at 4 °C. Then 0.8 mL of supernatant was added to 0.1 mL of 50% H_2SO_4 and 0.8 mL of extracting solution (25 mg L^{-1} stock in methyl *tert*-butyl ether) as the internal standard, vortex mixed for 10 s, oscillated for 10 min, and ultrasound treated for 10 min (ice water bath). The sample was centrifuged at 10 000 rpm for 15 min at 4 °C, and incubated at −20 °C for 30 min. The supernatant was taken out into the sample vial for GC-MS detection.

Short-chain fatty acids (SCFAs) were analyzed by gas chromatography-mass spectrometry (GC-MS) (GC2030-QP2020 NX system, Shimadzu Corporation, Japan), as previously described.[22] The system was equipped with an HP-FFAP capillary column (30 m × 250 μm × 0.25 μm) (J&W Scientific, Folsom, CA, USA). The carrier gas was helium. The flow of helium was set at 3.0 mL min^{-1} with a split ratio of 5 : 1. The volume of sampling was 1 μL at the temperature of 240 °C. The ionization temperature was 240 °C. The concentration of SCFAs (μmol g^{-1}) was calculated according to the standard curve obtained by the external standard method.

2.12. Non-targeted metabolomic analysis of rat blood

100 μL of blood sample and 400 μL of extraction solution (methanol : acetonitrile = 1 : 1 (v/v)) were mixed. The extraction solution contained the internal standard for isotope labeling. The mixture was swirled for 30 s, ultrasonicated for 10 min, and incubated at −40 °C for 1 h. The sample was centrifuged at 13 800*g* for 15 min at 4 °C. The supernatant was transferred to a fresh glass vial for analysis. The quality control (QC) sample was prepared by mixing an equal aliquot of the supernatant of samples.

This study utilized the Thermo Vanquish ultra-high-performance liquid chromatographic system and Waters ACQUITY UPLC BEH Amide liquid chromatography column (2.1 mm × 50 mm, 1.7 μm). Phase A was aqueous, containing 25 mmol L^{-1} ammonium acetate and 25 mmol L^{-1} ammonia. Phase B was acetonitrile. The sample tray temperature was 4 °C and the sample volume was 2 μL. The Orbitrap Exploris 120 mass spectrometer was controlled using a control software (Xcalibur, version 4.4, Thermo) for primary and secondary mass spectrometry data acquisition. The detailed parameters are as follows: sheath gas flow rate: 50 Arb; aux gas flow rate: 15 Arb; capillary temperature: 320 °C; full MS resolution: 60 000; MS/MS resolution: 15 000; collision energy: SNCE 20/30/40; and spray voltage: 3.8 kV (positive) or −3.4 kV (negative). After the original data were converted into mzXML format using the ProteoWizard software, metabolite identification was carried out using the co-authored R package, the database was BiotreeDB (V3.0), and the visualized analysis was carried out using the self-authored R package.

2.13. Statistical analysis

All statistical analyses were performed using Origin 8.5. The data are presented as the mean ± SD for each group. The differences between the mean values of the groups were analyzed by one-way analysis of variance with Tukey's HSD test. The ana-

lyses were performed using SPSS software. A p value of less than 0.05 was considered to indicate statistical significance.

3. Results

3.1 Effect of probiotics on arthritis symptoms in CIA rats

The paws of normal rats were plump in shape, glossy in color, full in texture and powerful in stretching (Fig. 2A). The first and booster immunizations resulted in redness and swelling of the paw, along with distortion of the toe and ankle joints (Fig. 2B). This redness and distortion were alleviated by the oral administration of probiotics, particularly in the *L. acidophilus* group (Fig. 2C–G). We further assessed the rats' body weight, clinical arthritis score, and paw thickness to quantitatively evaluate the severity of RA in the rats. In Fig. 2H, under the action of two immunizations, the weight of the rats decreased in the 4th week. In the 6th week of probiotics, the weight of the rats resumed the upward trend again. However, the body weight of the CIA model group of rats continued to decline at the 6th week. The significant difference analysis of body weight between groups is shown in Table S1.† The clinical arthritis scores (Fig. 2I) indicated that the symptoms of arthritis in the rats escalated rapidly in the 5th week and entered the acute stage of disease. Nevertheless, under the action of probiotics, this acute growth phenomenon disappeared, particularly in the *L. acidophilus* group. The significant difference analysis of clinical arthritis scores between groups is shown in Table S2.† As shown in Fig. 2I, the clinical scores of arthritis in the *L. casei* group, *L. reuteri* group and *Bifidobacterium* group were similar, while those in the *L. acidophilus* group were similar to those in the MTX group. Similarly, the *L. acidophilus* group exhibited a significant reduction in paw swelling thickness ($p < 0.05$) (Fig. 2J). The significant difference analysis of paw thickness between groups is shown in Table S3.† In addition, the results of H&E staining and safranin O-fast green staining showed that treatment with MTX and probiotics did not prevent the loss of the cartilage matrix. These results are included in the ESI.†

3.2 Effect of probiotics on expression of TNF-α and MMP-13 in the knee tissue of CIA rats

To further assess inflammation in the knee joints of CIA rats, we evaluated the expression of TNF-α and MMP-13 in joint tissues using specific immunofluorescence staining. As shown in Fig. 4, no positive fluorescence signals were detected in the joint tissues of control rats. In contrast, the CIA model group exhibited prominent fluorescence markings. Positive fluo-

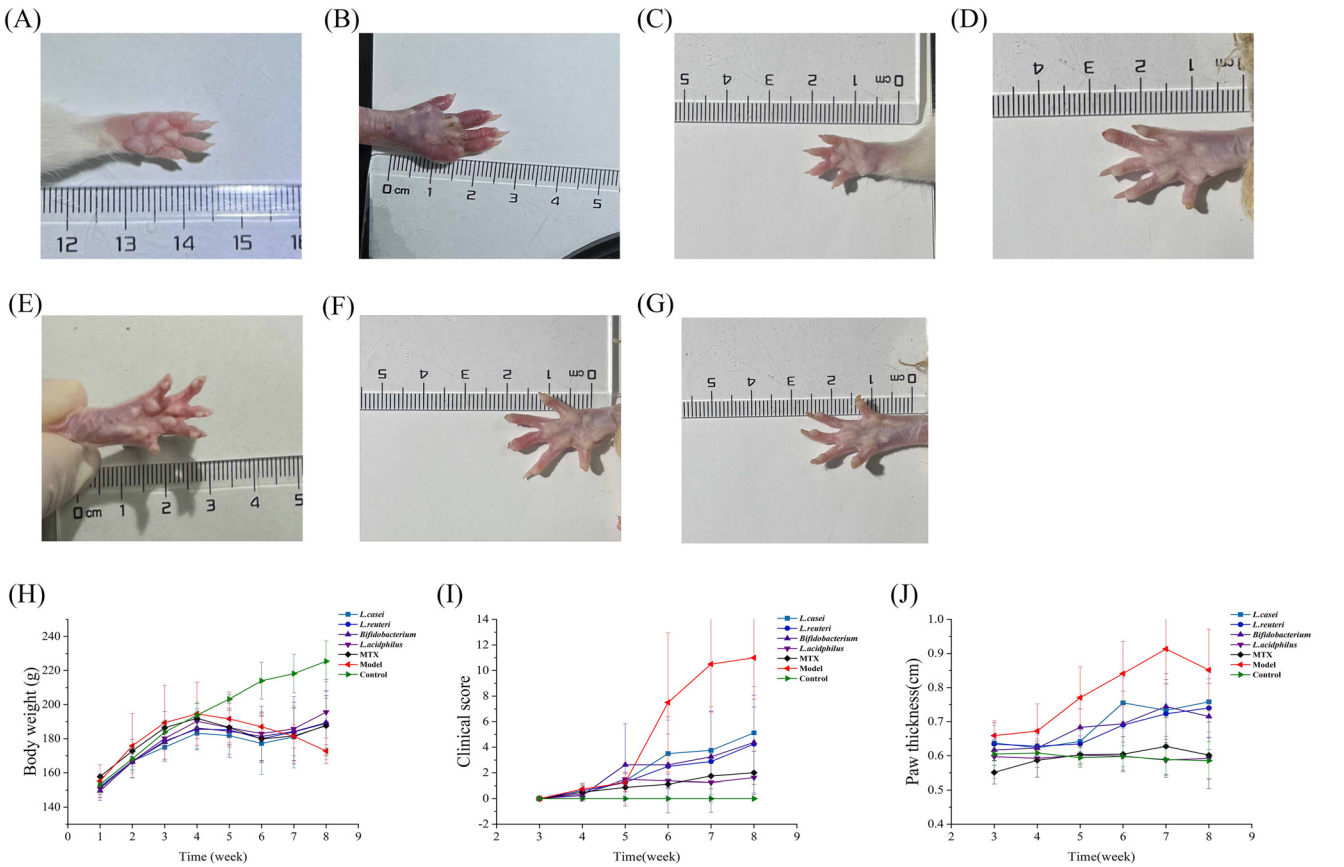

Fig. 2 Effect of probiotics on CIA rats. (A) Control, (B) CIA model, (C) MTX, (D) *L. casei*, (E) *L. reuteri*, (F) *Bifidobacterium*, (G) *L. acidophilus*, (H) body weight of each group of rats, (I) clinical scores of arthritis in each group of rats, (J) Paw thickness of each group of rats.

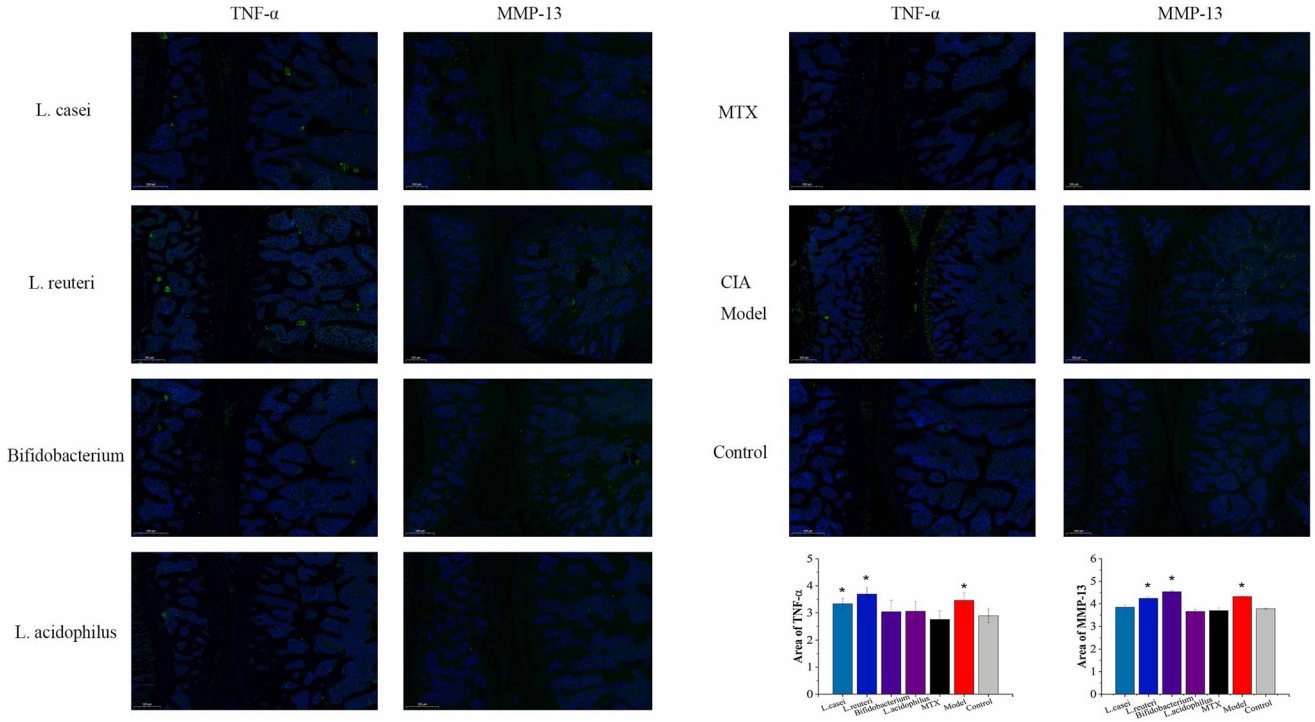

Fig. 3 Comparison of the distribution of MMP-13 and TNF-α in the joint tissues of each group.

rescence signals were also detected in each probiotic group. To quantitatively compare the fluorescently labeled areas among the groups, we utilized ImageJ image processing software for analysis, with the results presented in the column diagram in Fig. 3. The fluorescence signal areas for TNF-α and MMP-13 in the knee joints of the CIA model group were significantly greater than those in the control group ($p < 0.05$). After oral administration of probiotics, the expression level of TNF-α in the *Bifidobacterium* group and *L. acidophilus* group was not significantly different from that in the control group. The expression level of MMP-13 in the *L. casei* group and *L. acidophilus* group was not significantly different from that in the control group. Therefore, based on the above results, only the *L. acidophilus* group could significantly reduce the expression levels of TNF-α and MMP-13 in the knee joints of CIA rats, reflecting the effect of the *L. acidophilus* group on reducing knee joint inflammation.

3.3 Effect of probiotics on CIA rat autoantibodies

Autoantibodies serve as a crucial index in the clinical diagnosis of RA. Anti-CII IgG antibodies are specific to CII and can induce or exacerbate arthritis. Reducing the production of these autoantibodies can effectively impede the progression of arthritis. In this section, we measured the concentrations of anti-CII IgG and its subtypes (anti-CII IgG1, anti-CII IgG2a, and anti-CII IgG2b) in the serum of rats to evaluate the impact of probiotics on humoral immunity in CIA models. In Fig. 4A–D, the serum levels of total anti-CII IgG, anti-CII IgG1, anti-CII IgG2a, and anti-CII IgG2b in the CIA model group are shown to be significantly elevated compared to those in the control group ($p < 0.05$). The MTX group exhibited a significant reduction in the titers of anti-CII IgG, anti-CII IgG1, anti-CII IgG2a, and anti-CII IgG2b in serum, with p values less than 0.01. Compared with the CIA model group, the *L. casei*, *Bifidobacterium* and *L. acidophilus* groups showed significantly decreased levels of anti-CII IgG, anti-CII IgG1, anti-CII IgG2a, and anti-CII IgG2b in the serum ($p < 0.05$ or 0.01). These findings suggest that *L. casei*, *Bifidobacterium* and *L. acidophilus* mitigate inflammatory damage induced by autoantibodies by inhibiting the levels of anti-CII IgG, anti-CII IgG1, anti-CII IgG2a, and anti-CII IgG2b, thereby regulating humoral immunity in CIA models.

3.4 Effect of probiotics on cytokines in CIA rats

Cytokines are highly sensitive to environmental factors and serve as important indicators for assessing the immune and inflammatory responses of the body. In this section, serum levels of IL-1β and IL-6 were measured to evaluate the systemic inflammatory immune response in rats. In Fig. 4E and F, the levels of pro-inflammatory factors (IL-1β and IL-6) in the CIA model group were significantly higher compared to the control group ($p < 0.001$). Both oral probiotics and MTX were found to significantly reduce serum cytokine levels (IL-1β and IL-6) ($p < 0.05$). Notably, the *L. reuteri* group and the *Bifidobacterium* group exhibited a significant reduction in IL-1β levels compared to the CIA model group ($p < 0.01$). Additionally, the *L. reuteri* group and the *L. acidophilus* group demonstrated a significant decrease in IL-6 levels compared to the CIA model

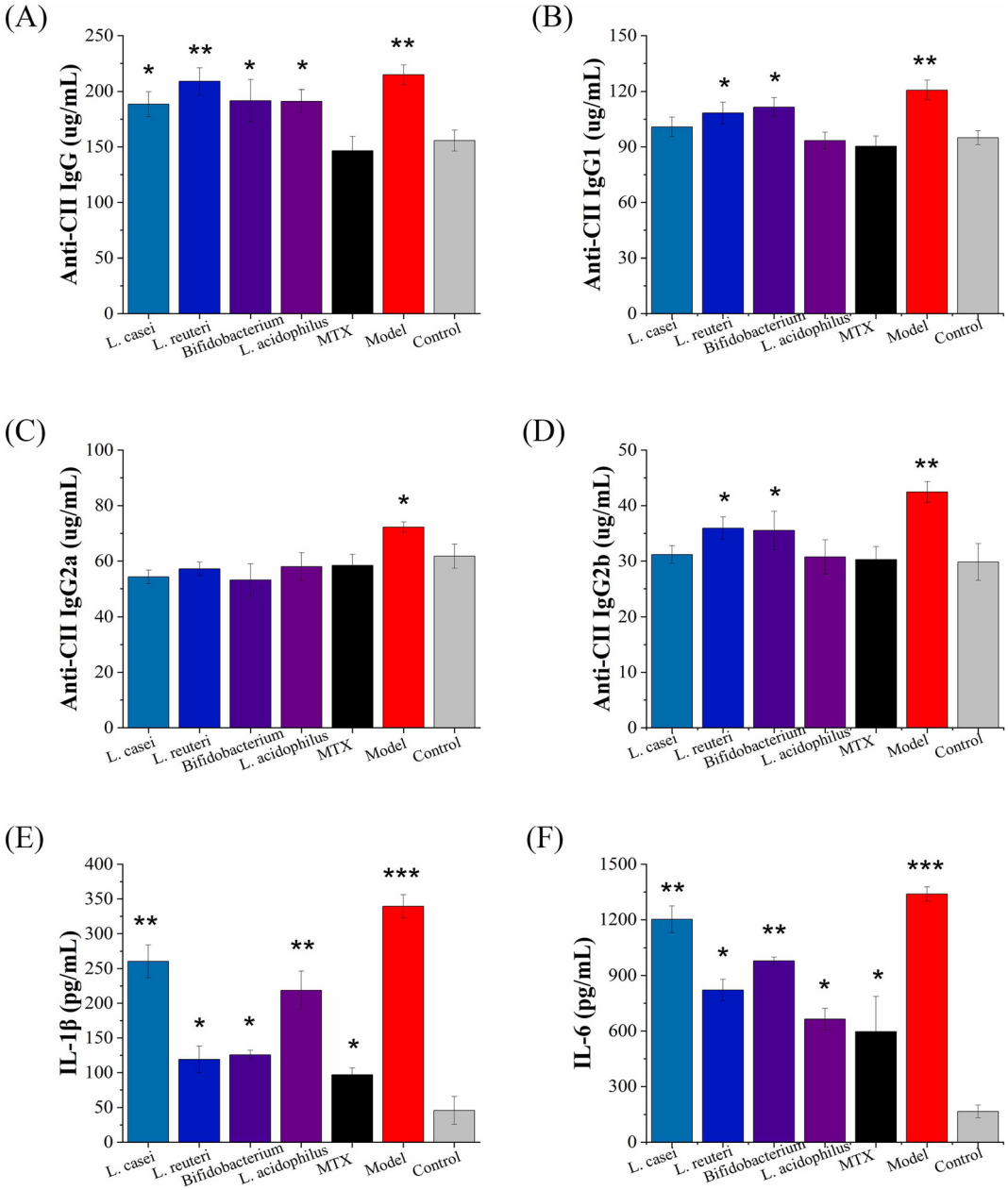

Fig. 4 Effects of probiotics on autoantibodies and cytokines in CIA rats. The levels of total anti-CII IgG (A), anti-CII IgG1 (B), anti-CII IgG2a (C), anti-CII IgG2b (D), IL-1β (E) and IL-6 (F) in serum were determined in each group. ** means $p < 0.01$, * means $p < 0.05$ against the control group.

group ($p < 0.01$). Pro-inflammatory factors play an important role in initiating or directly mediating the activation of leukocytes, promoting the activation of osteoclasts, stromal cells and chondrocytes, and inducing joint injury. The results of this study also reflect the effect of probiotics to reduce inflammation in the body.

3.5 Effect of probiotics on the gut microbiota of CIA rats

Using 16S rDNA V3–V4 sequencing technology, we analyzed α-diversity, β-diversity, and the composition of intestinal microorganisms to investigate the regulatory effects of probiotics on the gut microbiota of CIA rats. The rank abundance curve (Fig. 5A) and rarefaction curves (Fig. 5B and C) indicate that the curves approach a flat line, suggesting that the sequencing depth is adequate to reflect the species richness of the samples. We further assessed the significant differences in species richness among the groups using violin plots based on the Chao1, observed species, and Shannon indices (Fig. 5D–F). As shown in Fig. 5D–F, CIA did not result in a significant difference in the α-diversity of intestinal microbiota in the rats ($p > 0.05$). However, the oral administration of *Bifidobacterium* led to significant differences in the α-diversity of the gut microbiota between the *Bifidobacterium* group and the other groups ($p > 0.05$).

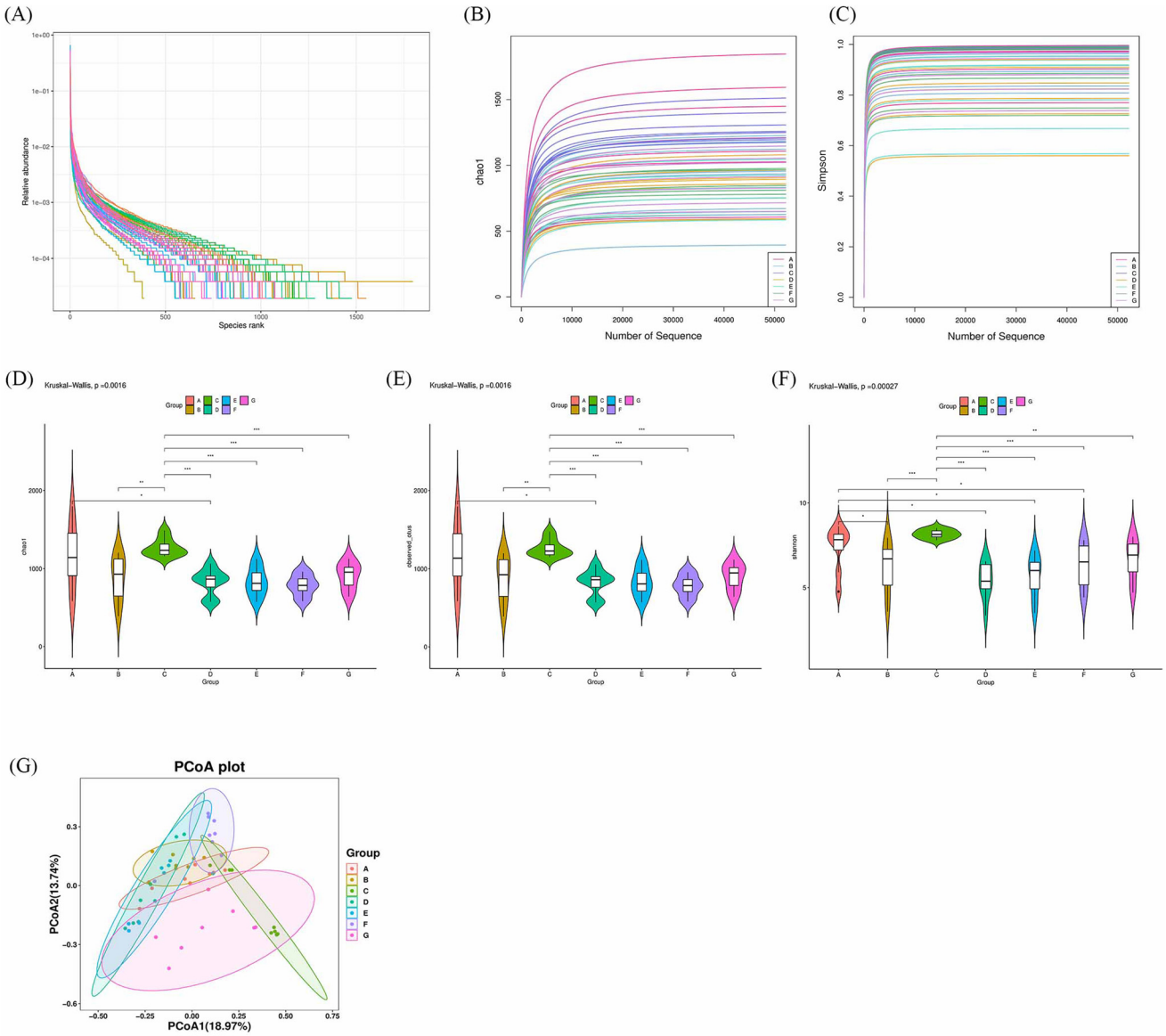

Fig. 5 Effects of probiotics on α-diversity and β-diversity of the gut microbiota in CIA rats. (A) Rank abundance curve, (B) Chao1 rarefaction curve, (C) Simpson rarefaction curve. In α-diversity analysis, Chao1 index (D), observed OTUs (E) and Shannon index (F) were selected to draw the violin plots. The upper left corner of the violin plots shows the rank and *p*-value obtained by the test for each group. *** means $p < 0.001$, ** means $p < 0.01$, * p means < 0.05. In β-diversity analysis, PCoA based on the Bray–Curtis distance (G). Group A: *L. casei*, Group B: *L. reuteri*, Group C: *Bifidobacterium*, Group D: *L. acidophilus*, Group E: MTX, Group F: CIA model, Group G: Control.

We further analyzed β-diversity among groups using principal coordinate analysis (PCoA). As can be seen from Fig. 5G, the species profiles were different between the CIA model group (purple circle) and the control group (pink circle). The CIA model group (purple circle) and the control group (pink circle) are two separate circles, indicating that CIA makes a significant difference in the β-diversity of rat gut microbiota. Under the action of MTX (blue circle) in Fig. 5G, the species profile is tilted towards the control group. After oral administration of probiotics (*L. casei*, *L. reuteri*, *Bifidobacterium* and *L. acidophilus*), the species profile of the gut microbiota of CIA rats also changed. It is noteworthy that the species profiles of the *L. acidophilus* group are closely aligned with those of the MTX group.

To evaluate species abundance across different groups and assess the similarity between them, Bray–Curtis distance was employed for sample clustering analysis. At the phylum level, the relative abundances of *Firmicutes*, *Bacteroidota*, *Proteobacteria* and *Patescibacteria* varied between the CIA model group and the control group (Fig. 6A). The relative abundance of each phylum in each probiotic group also changed. According to the histogram (Fig. 6A), the distribution ratio of each phylum in the *Bifidobacterium* group was the closest to that in the control group, while the difference

between the *L. reuteri* group and the control group was the greatest. The significant difference analysis revealed that the relative abundances of *Bacteroidota* and *Verrucomicrobiota* in the CIA model group were significantly lower than those in the control group, while the relative abundances of *Patescibacteria* and *Actinobacteriota* in the CIA model group were significantly higher than those in the control group (Fig. 6B). By comparing the results of probiotic groups, the relative abundances of *Patescibacteria* and *Actinobacteriota* in the *L. acidophilus* group were significantly lower than those in the CIA model group (Fig. 6C). At the genus level, the relative abundances of *Muribaculaceae*_unclassified, *Ligilactobacillus*, *Streptococcus* and *Prevotellaceae* in the CIA model group were significantly lower than those in the control group. Conversely, the relative abundances of *Lactobacillus*, *Clostridia*_UCG-014_unclassified, *Ruminococcus*, and *Candidatus_Saccharimonas* in the CIA model group were significantly higher than those in the control group (Fig. 6D and E). Among the probiotic groups, the distribution ratio of bacteria in the *L. casei* group was the closest to that in the control group, while the difference between the *Bifidobacterium* group and control group was the largest. By comparing the results of the probiotic groups, we observed that the relative abundance of *Ligilactobacillus* in the *L. acidophilus* group was significantly higher than that in the CIA model group. Conversely, the relative abundances of *Lactobacillus*, *Clostridia*_UCG-014, *Ruminococcus*, *Candidatus_Saccharimonas*, *Romboutsia*, *Turicibacter*, *Clostridium_sensu_stricto*_1, *Dubosiella*, *Erysipelotrichaceae*_unclassified, *Enterorhabdus* and *Adlercreutzia* in the *L. acidophilus* group were significantly lower than those in the CIA model group (Fig. 6F). In addition to *L. acidophilus*, gut microbial alterations of other probiotic groups are included in the ESI.† In summary, both the control group and the *L. acidophilus* group exhibited similar changes in the relative abundance of these microorganisms at both the phylum and genus levels, indicating the ability of *L. acidophilus* to restore the relative abundance of intestinal microorganisms in CIA rats. The bubble plot in Fig. 6G further corroborated our experimental findings.

Furthermore, we employed LEfSe (LDA Effect Size) analysis to identify microbiota with significant differences in abundance, referred to as biomarkers, among the various groups. As illustrated in Fig. 7A, the CIA model group, control group, and *L. acidophilus* group each exhibit distinct biomarkers. At the phylum level, the biomarkers for the CIA model group were *Patescibacteria* and *Actinobacteriota*, while those for the control group included *Bacteridota* and *Verrucomicrobiota*. The *L. acidophilus* group was characterized by the presence of *Firmicutes* at the phylum level. Further taxonomic subdivision revealed that the biomarkers of the CIA model group included *Lactobacillus*, *Clostridia*_UCG_014, *Candidatus_Saccharimonas*, *Ruminococcus*, *Romboutsia* and *Eubacterium_xylanophilum*_group. In contrast, the control group displayed biomarkers such as *Bacteroidales*, *Muribaculaceae*, *Streptococcus*, *Prevotellaceae*, *Parabacteroides*, *Akkermansiaceae*, *Butyricicoccaceae*, *Erysipelatoclostridium* and *Clostridia*_UCG_014. The biomarkers of the *L. acidophilus* group comprised *Ligilactobacillus*, *Lactobacillaceae*, *Rikenellaceae*_RC9_gut_group, *Bacteroidota* and *Eubacterium*.

Based on the functional annotation results from the KEGG database, PICRUSt2 was employed to map the microbiota and predict functional differences arising from variations in these biomarkers. As illustrated in Fig. 7B, the biomarkers in the CIA model group resulted in significant alterations in energy metabolism and carbon fixation in photosynthetic organisms. Furthermore, the intervention with *L. acidophilus* notably influenced purine metabolism, transcription factors, and pyruvate metabolism.

3.6 Effect of probiotics on the production of short chain fatty acids

We measured the production of SCFAs by the gut microbiota of rats in each group, and the results are presented in Fig. 8. As can be seen in Fig. 8A–F, acetic acid, propionic acid, and butyric acid are the three most abundantly produced SCFAs. The production levels of acetic acid, propionic acid, and butyric acid in the control group were significantly higher than those in the CIA model group ($p < 0.001$). Following the intervention with probiotic mixed strains (*L. casei* group, *L. reuteri* group, *Bifidobacterium* group, *L. acidophilus* group), the butyric acid content increased significantly compared to the CIA model group (Fig. 8C). Notably, the acetic acid content in the *Bifidobacterium* group and the *L. acidophilus* group also increased significantly relative to the CIA model group (Fig. 8A). Additionally, the propionic acid content in the *L. casei* group was significantly higher than that in the CIA model group (Fig. 8B). Conversely, iso-butyric acid, valeric acid, and iso-valeric acid were produced in lower quantities. The iso-butyric acid content was significantly different between the control group and the CIA model group, with the *Bifidobacterium* intervention leading to a significant decrease in iso-butyric acid levels compared to the CIA model group ($p < 0.001$) (Fig. 8D). However, no significant difference in valeric acid content was observed between the groups (Fig. 8E). Although significant differences in iso-valeric acid content were found between the control group and the CIA model group, neither probiotics nor MTX intervention resulted in significant changes in iso-valeric acid levels (Fig. 8F).

In summary, compared with other groups, the *L. acidophilus* group showed better performance in reducing the arthritis score and paw swelling, alleviating serum specific antibodies and pro-inflammatory factors, and restoring intestinal SCFA production. Therefore, in the next experiment, we took up the *L. acidophilus* group as the research object to determine whether one of the mixed strains plays the role or whether these strains play the role together.

3.7 Effect of a single strain of *L. acidophilus* on arthritis symptoms in CIA rats

To further investigate the potential role of mixed *L. acidophilus* strains in the prevention of RA, we separately grouped individual strains of *L. acidophilus* and conducted experiments on each strain sequentially. As shown in Fig. 9B, following

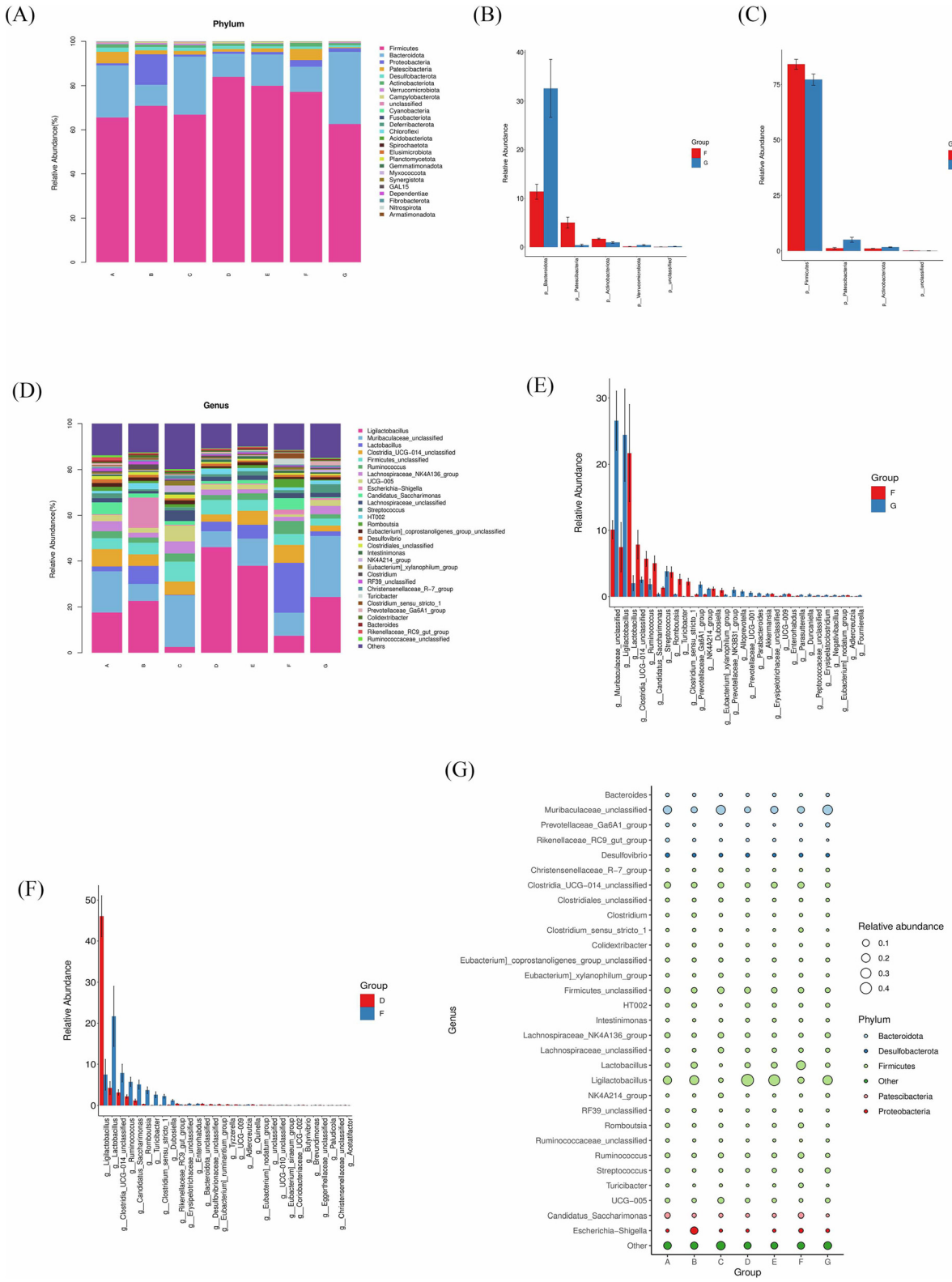

Fig. 6 Effects of probiotics on the relative abundance of the gut microbiota in CIA rats. (A) The relative abundance at the phylum level. (B) The relative abundance with significant difference between the CIA model group and control group at the phylum level. (C) The relative abundance with significant difference between the *L. acidophilus* group and CIA model group at the phylum level. (D) The relative abundance at the genus level. (E) The relative abundance with significant difference between the CIA model group and control group at the genus level. (F) The relative abundance with significant difference between the *L. acidophilus* group and CIA model group at the genus level. (G) Bubble plot of relative abundance distribution for each group. Group A: *L. casei*, Group B: *L. reuteri*, Group C: *Bifidobacterium*, Group D: *L. acidophilus*, Group E: MTX, Group F: CIA model, Group G: Control.

Fig. 7 Effects of *L. acidophilus* on the biomarkers and functions of the gut microbiota in CIA rats. (A) LEfSe difference analysis, (B) PICRUSt2 function prediction. Group D: *L. acidophilus*, Group F: CIA model, Group G: Control.

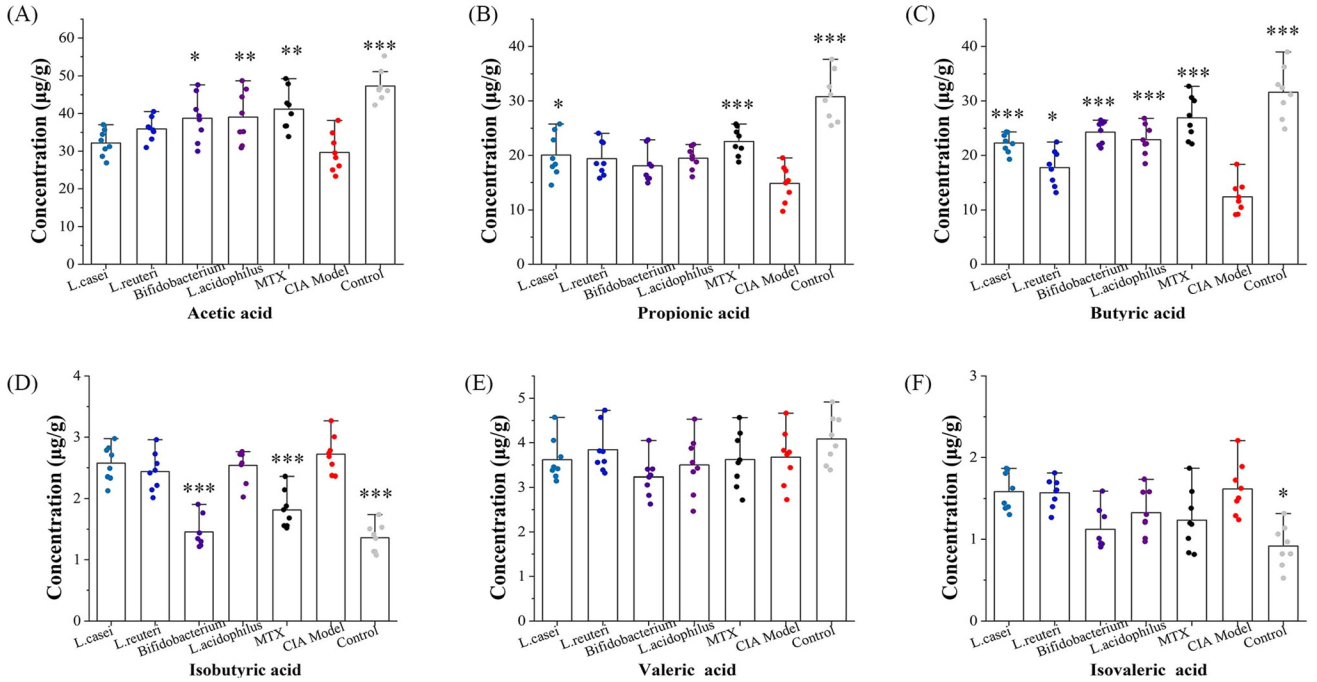

Fig. 8 Effects of probiotics on the production of short chain fatty acids of the gut microbiota in CIA rats. (A) acetic acid, (B) propionic acid, (C) butyric acid, (D) isobutyric acid, (E) valeric acid, (F) isovaleric acid. *** means $p < 0.001$, ** means $p < 0.01$, * means $p < 0.05$ against the CIA model group.

booster immunization, the rats developed red spots on their paws, with swelling extending across the entire sole of the foot. By the 6th week, joint inflammation and swelling in the rats peaked (Fig. 9J and K). The significant difference analysis of body weight, clinical score and paw thickness between groups is shown in Tables S4–S6.† These figures indicate that compared to the CIA model group, the paw thickness in both the NCFM and BD5032 groups was significantly reduced; however, the clinical score of arthritis did not show a significant decrease.

3.8 Effect of *L. acidophilus* on joint pathology in CIA rats

The effect of *L. acidophilus* on the degree of joint injury in rats was analyzed using H&E staining (left) and safranin O-fast green staining (right). Bovine collagen type II was injected into the rats to disrupt their immune tolerance, leading to the production of autoantibodies that target the synovial tissue. This process induced a local immune response in the joints and attracted a substantial number of inflammatory cells, resulting in the infiltration and inflammation of the synovial cells and subsequent destruction of the synovial membrane. In Fig. 10G, the CIA model group exhibited significant infiltration of synovial inflammatory cells, with the synovial layer fused to the bone interface. Treatment with DXMS (Fig. 10F) restored the infiltration of synovial inflammatory cells and synovial fusion in CIA rats to levels comparable to those of normal rats (Fig. 10H). Both *L. acidophilus* NCFM and *L. acidophilus* BD3545 were effective in decreasing the fusion between the synovial layer and the bone interface, thereby reducing joint bone tissue injury (Fig. 10B and D). Conversely, *L. acidophilus* BD18, *L. acidophilus* BD1802 and *L. acidophilus* BD5032 did not demonstrate a significant effect on the fusion of the synovial layer and bone interface (Fig. 10A, C, and E).

3.9 Effect of *L. acidophilus* on synovial inflammation in CIA rats

The expression and distribution of TNF-α and MMP-13 in joint tissues serve as indicators of the inflammatory response in rat joints. As shown in Fig. 11, no fluorescently labeled TNF-α protein signal was detected in the joint pathological sections of rats in the normal group, while a minor amount of fluorescently labeled MMP-13 protein signal was observed. In contrast, the CIA model group exhibited a substantial amount of fluorescently labeled MMP-13 protein, with only a small quantity of TNF-α protein being fluorescently labeled. Intervention with DXMS and *L. acidophilus* (BD18, NCFM, BD1802, BD3545, BD5032) led to a decrease in the levels of fluorescently labeled TNF-α and MMP-13 proteins. The ImageJ image processing software was utilized to quantitatively assess the fluorescence-labeled area and analyze significant differences. The histogram below demonstrates significant differences in the fluorescence signals of TNF-α and MMP-13 proteins between the control group and the CIA model group. Notably, DXMS was able to diminish the fluorescence signals of TNF-α and MMP-13 proteins in the CIA model group to levels that were not significantly different from those in the control group. Additionally, *L. acidophilus* BD3545 and *L. acidophilus* BD5032 significantly reduced the fluorescently labeled areas of the pro-

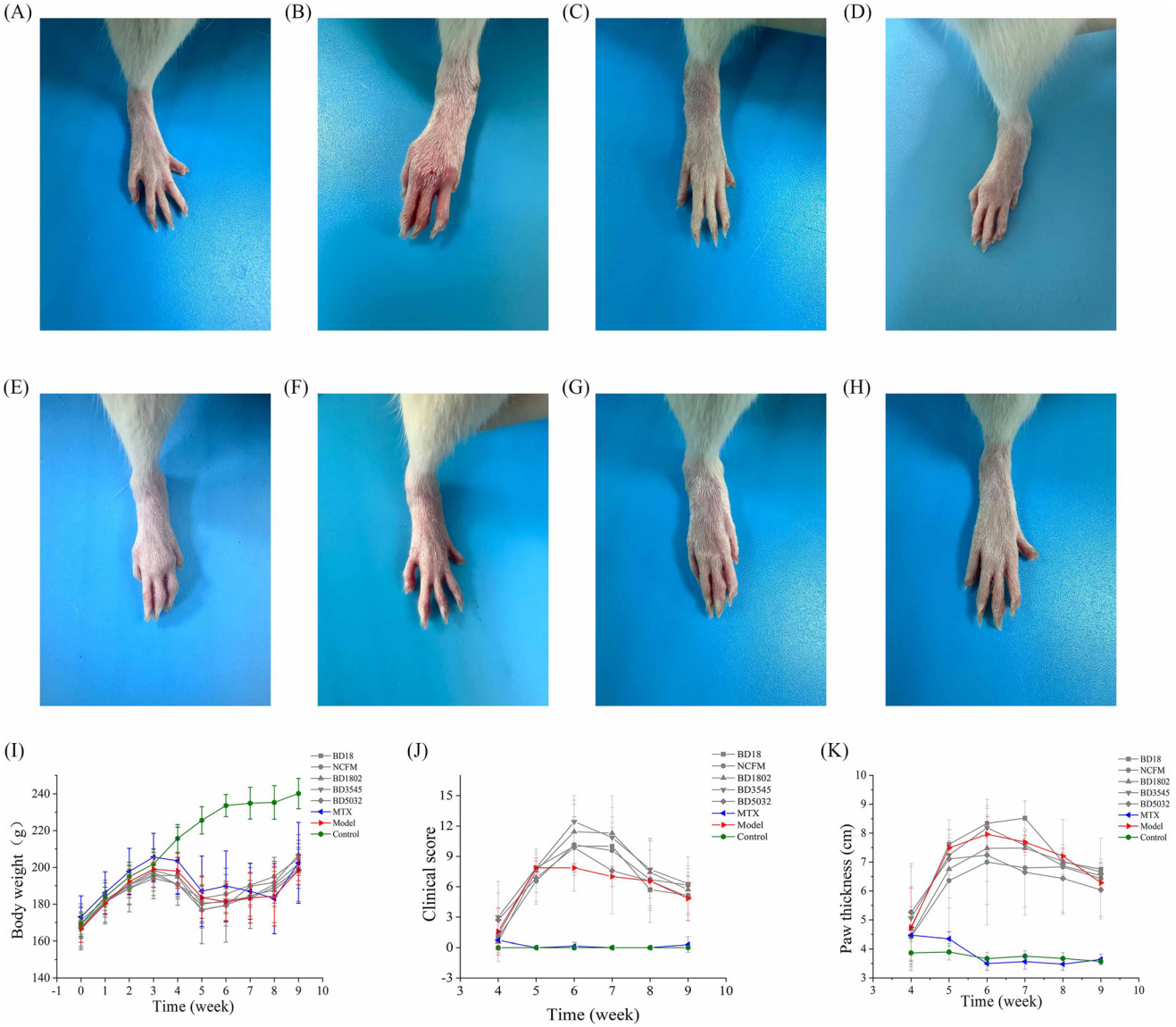

Fig. 9 Effects of oral treatment with *L. acidophilus* on rats with CIA. (A) Control, (B) CIA model, (C) DXMS, (D) BD18, (E) NCFM, (F) BD1802, (G) BD3545, (H) BD5032, (I) body weight of rats, (J) clinical score of arthritis, (K) Paw thickness of rats. *** means $p < 0.001$, ** means $p < 0.01$, * means $p < 0.05$ against the CIA model group. Abbreviation: DXMS, dexamethasone.

teins TNF-α and MMP-13 to levels comparable to those of the control group.

3.10 Effect of *L. acidophilus* on the gut microbiota of CIA rats

Using 16S rDNA sequencing technology, we analyzed α-diversity, β-diversity, and the composition of intestinal microorganisms to investigate the effects of *L. acidophilus* (including strains BD18, NCFM, BD1802, BD3545, and BD5032) on the gut microbiota of CIA rats. The rank abundance curve (Fig. 12A) and rarefaction curves (Fig. 12B and C) indicated that the sequenced sample data were reasonable and indirectly reflect the species richness of the samples. We employed the Chao1, Shannon, and Simpson indices to create a violin plot, which illustrated the influence of *L. acidophilus* on the α-diversity of the intestinal microbiota. Fig. 12D shows the differences in community richness between the control group and the CIA model group, with DXMS being able to restore the community richness of the intestinal microbiota in CIA rats to levels comparable to those of the control group. Notably, *L. acidophilus* strains BD3545 and BD5032 were found to decrease the community richness of the intestinal microbiota in CIA rats. As depicted in Fig. 12E and F, the community diversity of the intestinal microbiota in the CIA model group increased compared to the control group. Similarly, DXMS, along with *L. acidophilus* strains BD3545 and BD5032, was effective in reducing the elevated community diversity observed in CIA rats. To evaluate the impact of *L. acidophilus* on the β-diversity of the intestinal microbiota in CIA rats, we performed principal coordinates analysis (PCoA) based on the Jaccard distance (Fig. 12G), as well as analysis of similarities

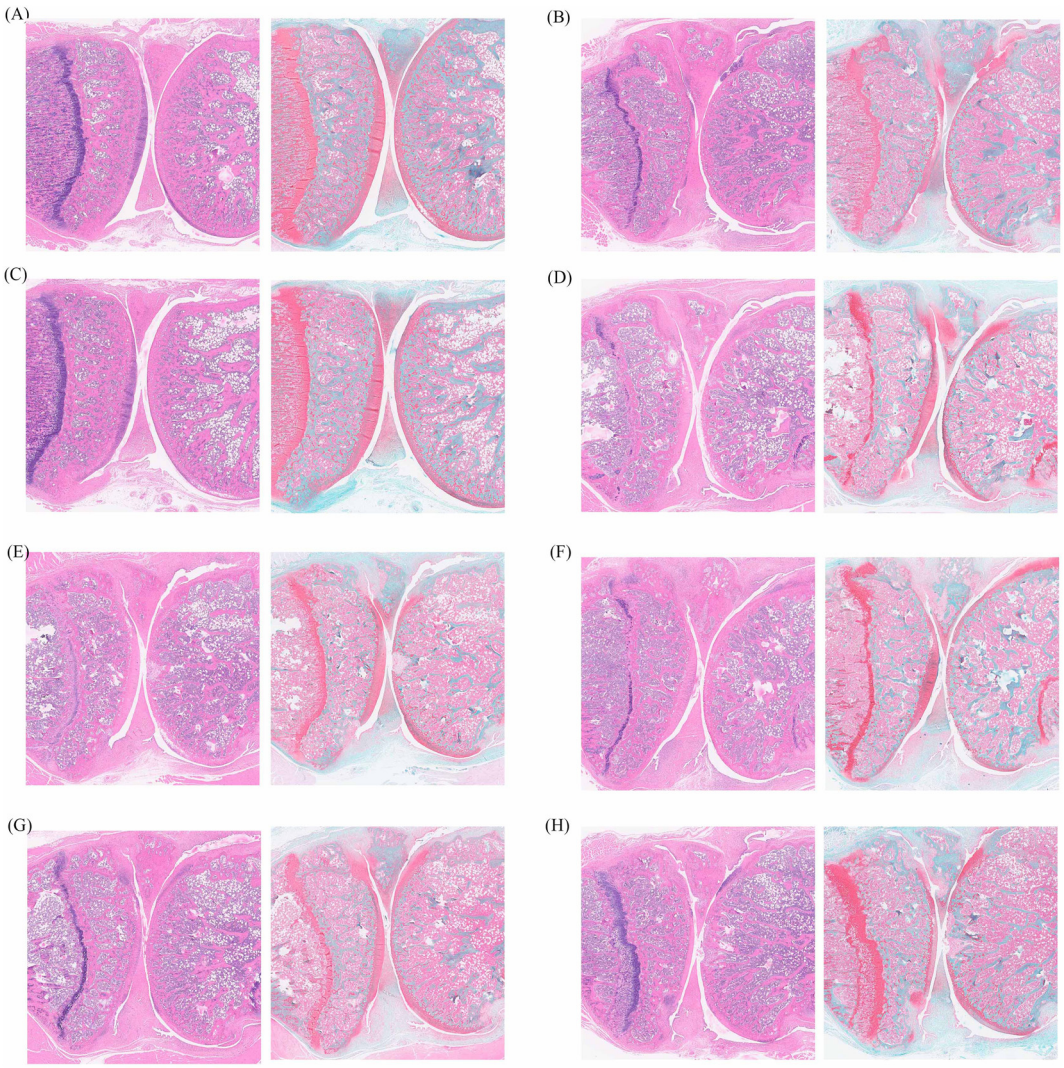

Fig. 10 Effects of oral treatment with *L. acidophilus* on histological changes of the knees joint in CIA rats. (A) Control, (B) CIA model, (C) DXMS, (D) BD18, (E) NCFM, (F) BD1802, (G) BD3545, (H) BD5032. Abbreviation: DXMS, dexamethasone. Score bar = 500 μm.

(ANOSIM) based on the Bray–Curtis distance (Fig. 12H) and unweighted UniFrac distance (Fig. 12I). In Fig. 12G, compared with the *L. acidophilus* group, the species profiles of the control group and the CIA model group overlapped less, and the species profiles of the control group completely covered the DXMS group. The species profiles of *L. acidophilus* group were different but not significant between the control group and the CIA model group. In Fig. 12H and I, there were differences between the control group and the CIA model group, which could be reduced by the effects of DXMS and *L. acidophilus* BD5032.

The detected amplicon sequence variants (ASVs) for each group were visually represented using Venn diagrams, as illustrated in Fig. 13A. In this figure, the control group exhibited the fewest unique ASVs, while the CIA model group displayed the second highest number of unique ASVs. Following the taxonomic profiling of ASVs, Venn diagrams were constructed at both the phylum level (Fig. 13B) and the genus level (Fig. 13C). At the phylum level, the control group had a greater number of unique ASVs compared to the CIA model group, which had fewer unique ASVs (Fig. 13B). Similarly, at the genus level, the control group again had more unique ASVs, while the CIA model group had fewer (Fig. 13C). To further investigate the differences and similarities among the samples, the Bray–Curtis distance was employed for clustering, and a stacked bar plot was created at both the phylum level (Fig. 13D) and genus level (Fig. 13F) to highlight the top 30 species based on abundance. The cluster tree structure on the left indicated that the species composition differed between the control group and the CIA model group at both the phylum and genus levels. At the phylum level (Fig. 13D), the species composition of the CIA model group closely resembled that of *L. acidophilus* BD5032. At the genus level (Fig. 13F), the CIA model group's composition was similar to that of *L. acidophilus* BD18, while the control group showed similarity to *L. acidophilus* BD3545. To synthesize the species compo-

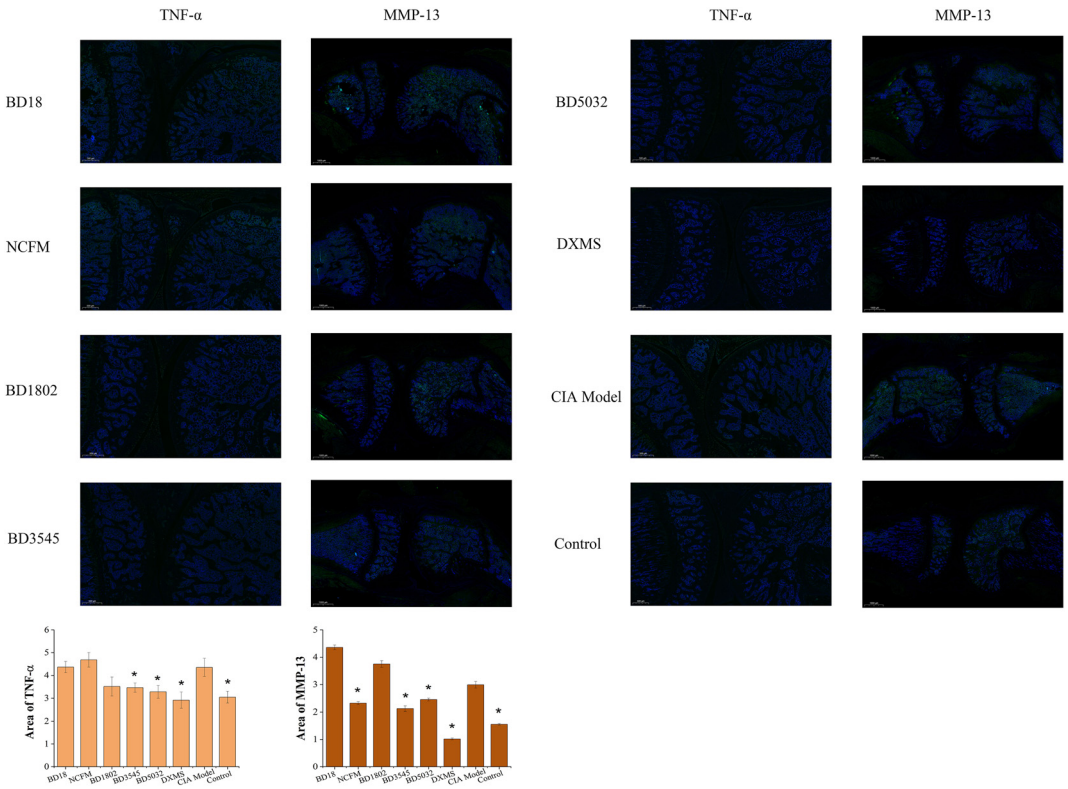

Fig. 11 The distribution of TNF-α and MMP-13 in rat joint tissues and their fluorescently labeled areas.

sition of each group at both the phylum and genus levels, a bubble plot was created, as shown in Fig. 13E. In this figure, the control group was characterized by a high relative abundance of the *Bifidobacterium* genus from the *Actinobacteriota* phylum, as well as the *Lactobacillus* and *Ligilactobacillus* genera from the *Firmicutes* phylum, with most genera originating from the *Firmicutes* phylum. Conversely, the CIA model group was characterized by a high relative abundance of the *Lachnospiraceae*_NK4A136_group genus and the *Lactobacillus* genus from the *Firmicutes* phylum, with a predominance of genera from the same phylum. Although the species composition of the *L. acidophilus* group did not closely resemble that of the control group, the composition of the *L. acidophilus* BD5032 group was similar to that of the DXMS group, with the relative abundance of the *Lactobacillus* genus from the *Firmicutes* phylum being highest in both the *L. acidophilus* BD5032 and DXMS groups.

As illustrated in Fig. 14A, *Lactobacillus*, *Ligilactobacillus*, HT002, *Bifidobacterium*, and *Akkermansia* were the predominant species. In the control group, *Bifidobacterium* was the dominant bacterium, comprising approximately 32% of the population. Conversely, in the CIA model group, *Ligilactobacillus* emerged as the dominant species, accounting for about 40%. *Lactobacillus* was identified as the predominant bacterium in DXMS, specifically *L. acidophilus* BD5032 and *L. acidophilus* BD1802. The dominant bacteria in *L. acidophilus* BD3545 and *L. acidophilus* BD18 included *Akkermansia*, *Lactobacillus*, and *Ligilactobacillus*. Notably, *L. acidophilus* NCFM exhibited a different profile, with *Ligilactobacillus*, HT002, and *Lactobacillus* as its dominant bacteria. According to the species evolutionary tree presented in Fig. 14B, *Lactobacillus*, *Ligilactobacillus*, and HT002 were closely related, all belonging to the *Firmicutes* phylum, while *Bifidobacterium* was classified under *Actinobacteriota*, and *Akkermansia* falls within *Verrucomicrobiota*. These findings indicate that CIA significantly reduced the relative abundance of *Bifidobacterium*, *Lactobacillus*, and HT002 in the intestinal microbiota of rats, while simultaneously increasing the relative abundance of *Ligilactobacillus*. Furthermore, *L. acidophilus* BD5032 and DXMS contributed to an increase in *Lactobacillus* within the intestinal microbiota of rats, with *L. acidophilus* BD5032 and *L. acidophilus* BD1802 also enhancing the levels of *Lactobacillus* and *Bifidobacterium*.

We further mapped the correlation heatmap based on the relationships among the dominant bacterial groups and the significant *p*-values obtained at the genus level. In Fig. 14C, *Bifidobacterium* exhibited a negative correlation with *Colidextribacter* and DNF00609. *Akkermansia* showed a negative correlation with *Candidatus_Saccharimonas* and *Escherichia. Shigella*. *Lactobacillus* was significantly negatively correlated with *Incertae_Sedis* and the *Eubacterium_siraeum*_group. *Desulfovibrio* demonstrated a positive correlation with both *Incertae_Sedis* and DNF00809. *Colidextribacter* was positively correlated with DNF00809, *Incertae_Sedis*, and *Desulfovibrio*. The *Eubacterium_xylanophilum*_group was positively correlated with *Desulfovibrio*. Additionally, *Escherichia_siraeum*_group was posi-

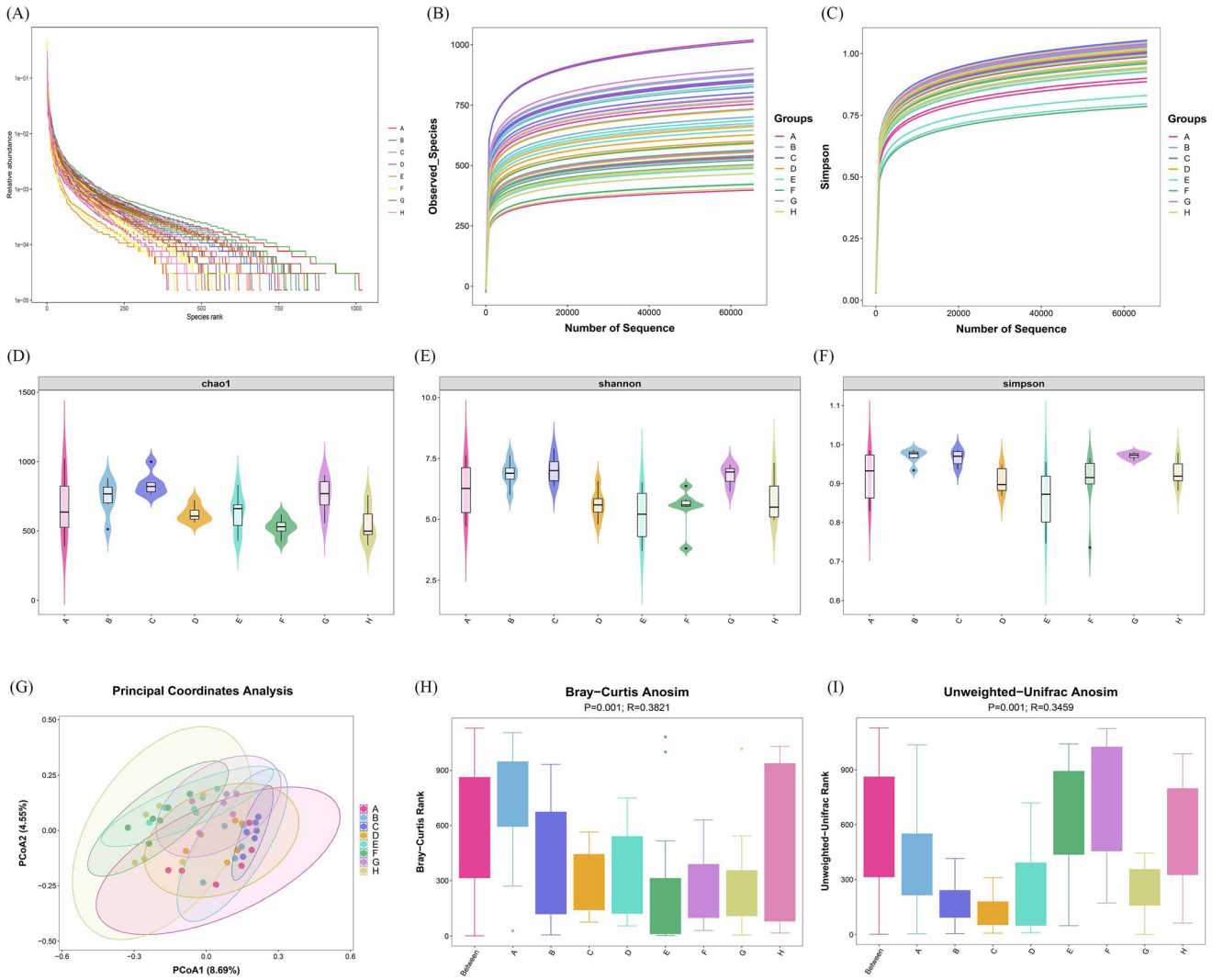

Fig. 12 Effects of oral treatment with *L. acidophilus* on histological changes of the knees joint in CIA rats. (A) Rank-abandance curve, (B) Specaccum curve, (C) Simpson curve, (D) Chao1 index, (E) Shannon index, (F) Simpson index, (G) PCA, (H) Anosim based on Bray-Curtis distance, (I) Anosim based on unweighted-unfrac distance. Group: A: BD18, B: NCFM, C: BD1802, D: BD3545, E: BD5032, F: DXMS, G: CIA model, H: Control. Abbreviation: DXMS, dexamethasone.

tively correlated with both *Desulfovibrio* and *Colidextribacter*. Finally, the *Lachnospiraceae*_NK4A136_group exhibited a positive correlation with the *Eubacterium_xylanophilum*_group.

3.11 Effects of *L. acidophilus* on blood metabolites in CIA rats

We further assessed the production of metabolites in the blood of CIA rats to evaluate the effects of *L. acidophilus* (BD18, NCFM, BD1802, BD3545, BD5032) on their metabolism. As shown n Fig. 15A, significant differences in blood metabolites were observed between the control group and the CIA model group. Fig. 15B indicates that compared to the control group, the CIA model group exhibited 245 upregulated and 246 downregulated differential substances. The top 10 significantly upregulated and downregulated substances were selected to create a matchstick diagram (Fig. 15C). In this diagram, the significantly upregulated differential metabolites included alsterpaullone, zalcitabine, dehydrogingerdione, various lipids and lipid molecules (*e.g.*, PC (30 : 0), 1-palmitoyl-2-arachidonoyl-*sn-glycero*-3-phosphoserine, *N*-oleoyl-D-*erythro*-sphingosylphosphorylcholine, acetylcarnitine (Car (2 : 0)), and PC (15 : 0/22 : 4(7*Z*,10*Z*,13*Z*,16*Z*))), as well as organic acids and their derivatives (Val-Leu and *N*-acetylcarnosine). Conversely, the significantly downregulated differential metabolites included *N*-(4-methylphenyl)-2-thiophenecarboxamide, leflunomide, various lipids and lipid molecules (*e.g.*, PC (32 : 2), 1,2-dioleoyl-*sn-glycero*-3-phosphoethanolamine-*N*,*N*-dimethyl, 1-myristoyl-*sn-glycero*-3-phosphocholine (LPC (14 : 0/0 : 0)), 1-(1*Z*-octadecenyl)-2-(5*Z*,8*Z*,11*Z*,14*Z*-eicosatetraenoyl)-*sn-glycero*-3-phosphocholine, (2*E*,11*Z*)-5-[5-(methylthio)-4-penten-2-ynyl]-2-furanacrolein, and PC (42 : 11)), as well as organic acids and their derivatives (Thr-Val-Leu and Pro-Thr). KEGG annotation of

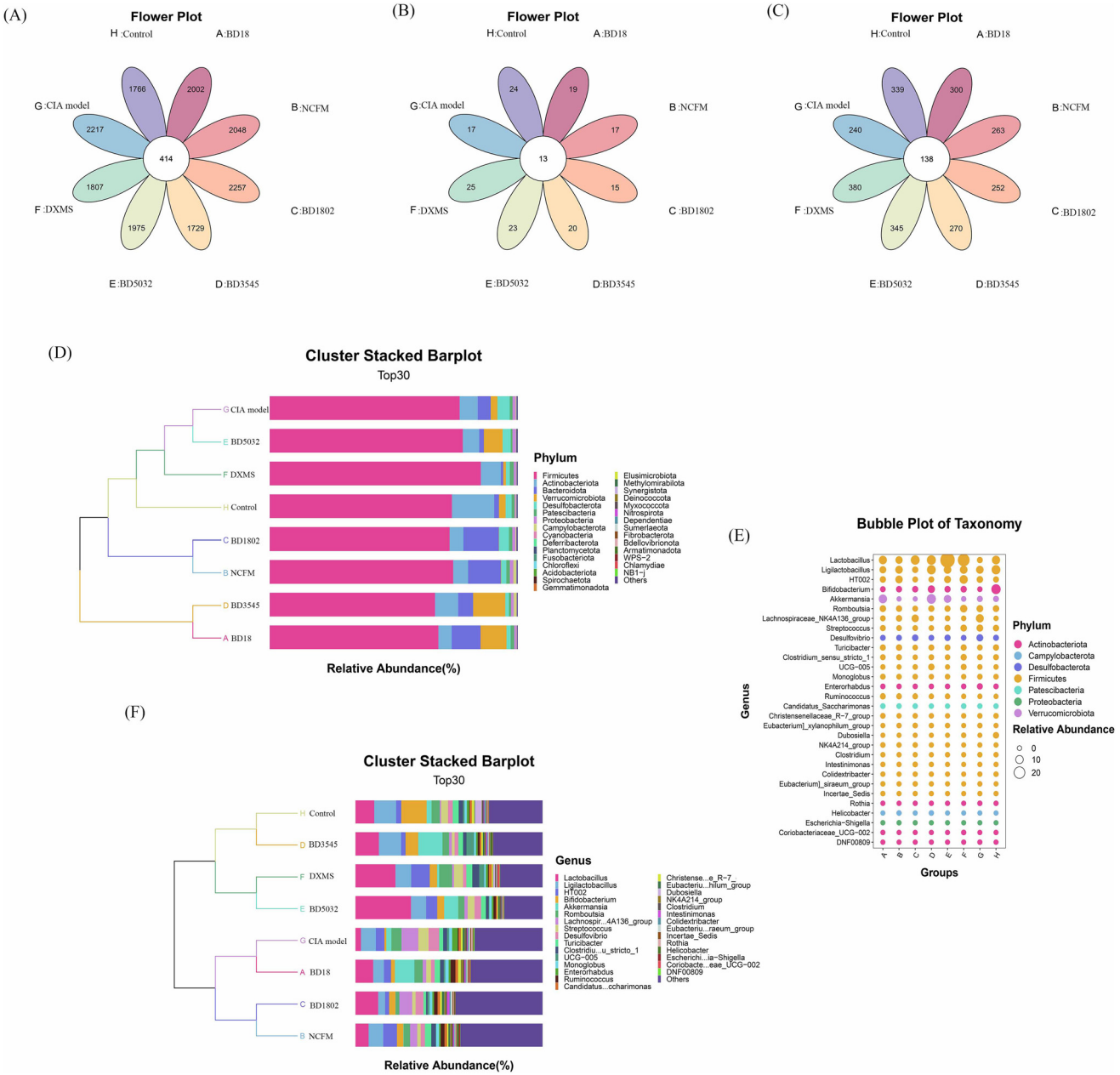

Fig. 13 Effects of oral treatment with *L. acidophilus* on the gut microbiota composition of CIA rats. (A) Venn diagram of the total ASVs, (B) Venn diagram of ASVs at the phylum level, (C) Venn diagram of ASVs at the genus level, (D) Cluster stacked barplot at the phylum level, (E) Bubble plot of taxonomy, (F) Cluster stacked barploy at the genus level. Group: A: BD18, B: NCFM, C: BD1802, D: BD3545, E: BD5032, F: DXMS, G: CIA model, H: Control.

these differential metabolites was conducted to derive the results of the related metabolic pathway analysis (Fig. 15D). The pathways significantly associated with these metabolites include arginine and proline metabolism, Vitamin B6 metabolism, pyrimidine metabolism, sphingolipid metabolism, alpha-linolenic acid metabolism, linoleic acid metabolism, and tryptophan metabolism, among others.

We further analyzed the correlation between the significantly different characteristic bacteria and the various metabolites to generate the heatmap presented in Fig. 15E. In this figure, *Akkermansia* exhibited a positive correlation with PC (18 : 0), 5-(tetradecyloxy)-2-furoic acid, 3-chloro-1*H*-indazole, and 3-acetyltyrosine. The *Lachnospiraceae*_NK4A136_group showed a positive correlation with 11-deoxyprostaglandin E2, hexadecatrienoylcarnitine (Car (16 : 3)), and phloroacetophenone_6[xylosyl-(1->6)-glucoside]. *Ruminococcus* was positively correlated with PC (18 : 0), apigenin 7-glucuronide, and DG (18 : 1(9*Z*)/18 : 4 (6*Z*,9*Z*,12*Z*,15*Z*)/0 : 0). Additionally, DNF00809 demonstrated a positive correlation with *N*-acetylphenylalanine.

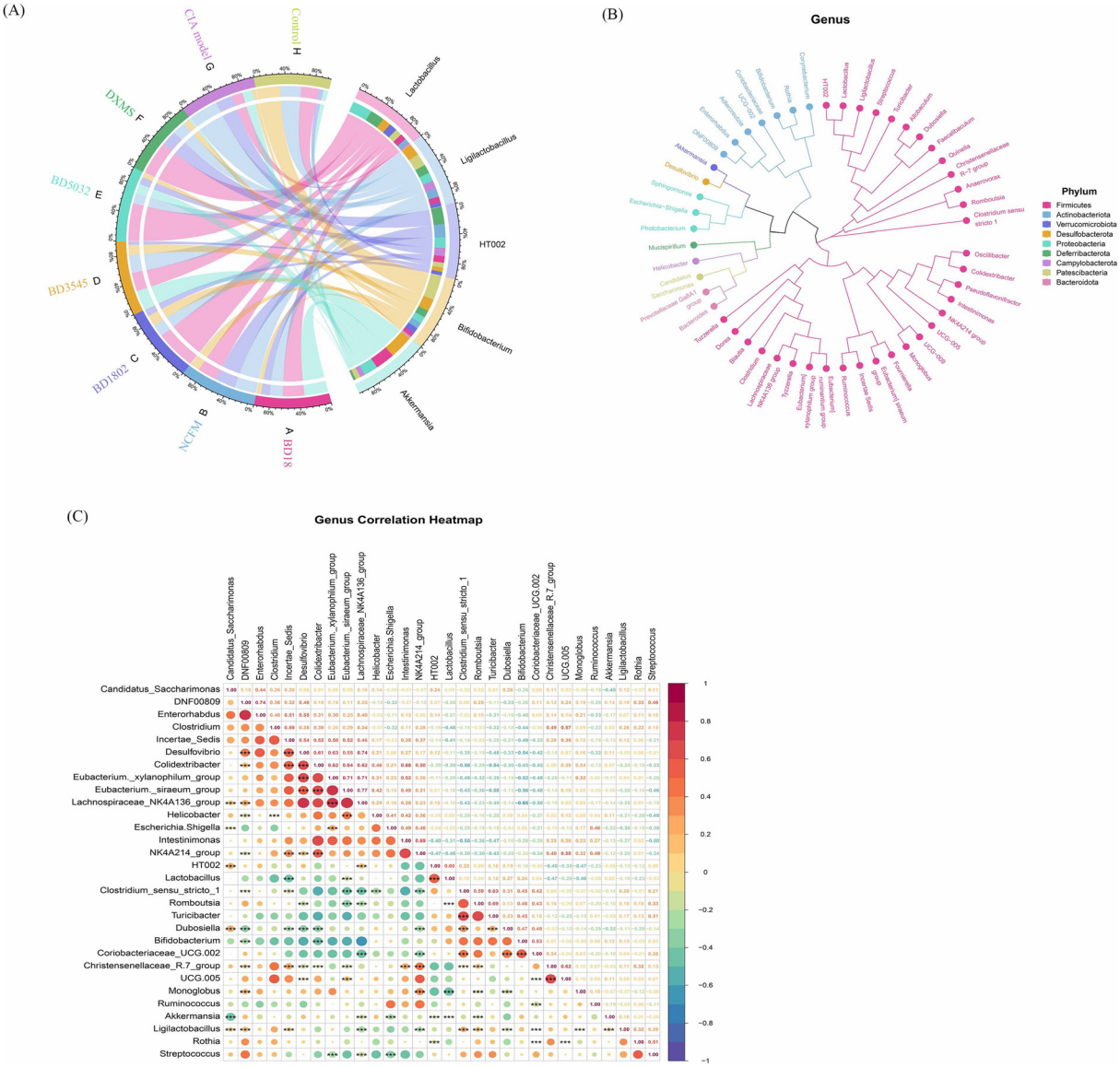

Fig. 14 Effects of oral treatment with *L. acidophilus* on the gut microbiota composition and correlation analysis of CIA rats. (A) Circos plot of the top5 genus, (B) Phylotree plot, (C) Gorrelation heatmap at the genus level. Group: A: BD18, B: NCFM, C: BD1802, D: BD3545, E: BD5032, F: DXMS, G: CIA model, H: Control.

4. Discussion

Rheumatoid arthritis (RA) is a chronic, symmetrical, systemic, inflammatory autoimmune disease.[1] The causes of RA mainly include genetic factors, microbial infections, hormonal stimulation, smoking, diet, and cold exposure.[23] Genetic susceptibility genes determine the body's vulnerability to the disease.[24] Microbial infection is considered to be the initial stage of RA; however, the mechanism of RA is still unclear.[25] Although there are corresponding drugs to treat RA, but there is still no effective treatment method, and in-depth studies of its etiology are expected to open up a new prospect for the treatment of RA.[26] More and more evidence shows that the occurrence and development of RA is closely related to local and systemic immune response disorders, and this RA immune abnormality originates from other immune sites outside the joint, which is the 'mucosal origin hypothesis'.[13,27,28] Mucosal immune system is an important part of the body's immune response.[29] The gut is considered to be the largest immune organ, and a large number of microorganisms exist in the gut.[30] The interaction, response and restraint between intestinal microorganisms and the intestinal mucosa—including the activation or inhibition of the adaptive immune system and the induced immune system of mononuclear phagocytes—are realized through the intestinal mucosal barrier.[31] The abundance of gut microbes indicates that the gut has the most antigenic substances, and changes in gut microbes can lead to changes in both local and systemic immune responses.

The mechanisms of gut microbiome involvement in autoimmune diseases remain unclear, but there is a large amount of

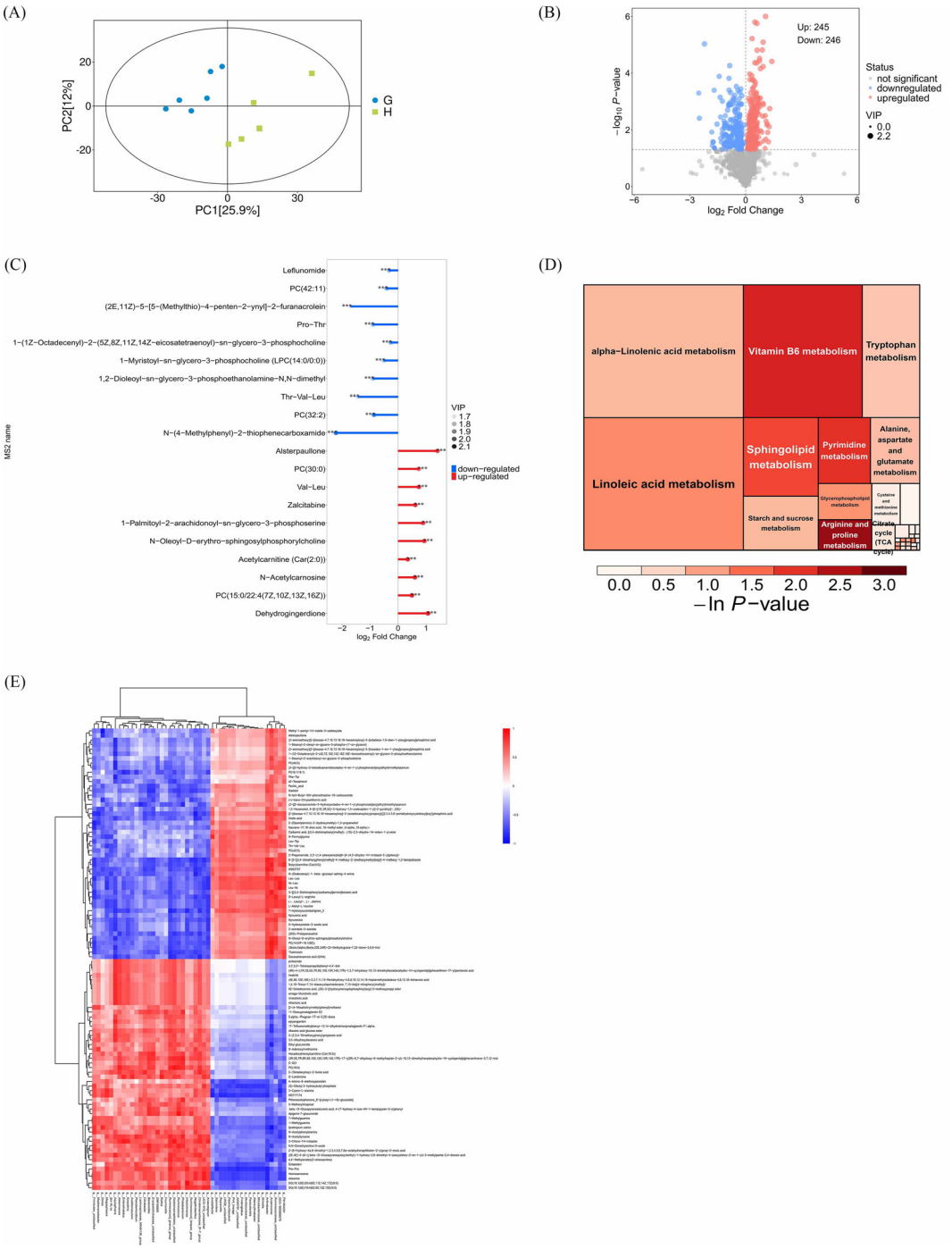

Fig. 15 Effects of oral treatment with *L. acidophilus* on the gut microbiota metabolites of CIA rats. (A) PCA plot of the CIA model group and control group. (B) Volcano plot of the CIA model group and control group. (C) Matchstick plot of the CIA model group and control group. (D) Tree map of the CIA model group and control group. (E) Heatmap of relation correlation analysis of characteristic bacteria genera and differential metabolites. Group G: CIA model; Group H: Control.

research evidence that the gut microbiome is involved in the occurrence and development of diseases. When gut microorganisms are in balance, the microorganisms in the gut do not induce an immune response.[32] However, once the balance of intestinal microbiota is broken, the normal microbiota will act as foreign invasion antigens. After the antigen presentation, lymphocytes are stimulated to proliferate and differentiate. Activated lymphocytes produce a variety of immune cytokines, such as IL-1, IL-2, and TNF-α. Under the influence of IL-1 and TNF-α, white blood cells migrate to the joint cavity and generate converge into the joint cavity and produce small inflammatory mediators, ultimately resulting in cartilage damage and bone

alterations.[32] In our study, the production of a large number of specific autoimmune antibodies and immune cytokines was detected in the blood of CIA rats. However, the specific antibodies anti-CII IgG1, anti-CII IgG2a, and anti-CII IgG2b, as well as the immune cytokines IL-1β and IL-6, were significantly decreased under the mixed strain of *L. acidophilus*. Based on the variations in antigens and cytokines, we further analyzed the gut microbiota of CIA rats using 16S sequencing. We observed an increase in the relative abundance of harmful bacteria, including *Clostridia*_UCG_014, *Candidatus*_*Saccharimonas*, *Streptococcus*, and *Clostridium*_*sensu*_*stricto*_1, in the CIA model group compared to the control group. A higher relative abundance of the symbiotic bacteria *Muribaculaceae*_unclassified and *Ligilactobacillus* was detected in the control group, compared with those of the CIA model group. Increased relative abundance of *Streptococcus* and *Clostridium*_*sensu*_*stricto*_1 has also been reported in the stools of American individuals with RA.[33] And it has been found in a number of other disease studies that increased relative abundance of *Clostridia*_UCG_014 is associated with several diseases, such as cough,[34] Alzheimer's disease,[35] and Parkinson's disease.[36] By reducing the relative abundance of intestinal *Candidatus*_*Saccharimonas*, muscle injury in mice caused by high-intensity exercise was alleviated.[37] The imbalance of harmful bacteria is indeed closely related to the occurrence and development of diseases. It is worth noting that the relative abundance of *Lactobacillus*, a common probiotic, was higher in the CIA model group than in the control group. Not only in our study, but also in other studies, the result was observed, for example studies on Chinese RA patients,[38] Italian RA patients[39] and Belgian RA patients.[40] A study by Liu *et al.*[38] demonstrated that increases in *Lactobacillaceae* and *Lactobacilli* were also measured in the gut microbiota of collagen-induced arthritis susceptible mice. This result is associated with drug resistance in mice, suggesting that these bacteria are predisposed to the disease.[38] In addition, excessive amounts of *Lactobacillus salivary* are present in both the gut and mouth of RA patients. The abundance of *Lactobacillus salivary* is higher in RA patients with more severe disease. *Bacillus* (especially *Lactobacillus*) are generally considered host friendly bacteria. However, some *Lactobacillus* such as *L. rhamnosus* GG and *L. reuteri* failed to ameliorate the disease in RA patients,[41–43] which suggests that different *Lactobacillus* species may have different effects on RA.

In this study, the intervention of *L. acidophilus* restored these unbalanced gut microbiomes. For instance, the relative abundance of beneficial bacteria such as *Ligilactobacillus*, *Lactobacillus*, *Romboutsia*, and *Ruminococcaceae*_unclassified, as well as harmful bacteria like *Clostridia*_UCG_014, *Clostridium*_*sensu*_*stricto*_1, and *Candidatus*_*Saccharimonas*, was found to recover, approaching the relative abundance levels observed in the control group (Fig. 7). However, in the screening tests of single strains of *L. acidophilus*, every single strain only seems to play a role in a certain RA evaluation index. For example, *L. acidophilus* NCFM and *L. acidophilus* BD5032 significantly reduced the paw thickness in CIA rats. Additionally, *L. acidophilus* NCFM and *L. acidophilus* BD3545 diminished the fusion between the synovial layer and the bone interface, while also mitigating damage to joint bone tissue. Furthermore, *L. acidophilus* BD3545 and *L. acidophilus* BD5032 significantly lowered the expression levels of TNF-α and MMP-13 proteins. These findings suggest that while *L. acidophilus* NCFM, *L. acidophilus* BD3545, and *L. acidophilus* BD5032 can each reduce specific RA indices in CIA rats, no single strain was capable of alleviating all RA symptoms. Each strain of *L. acidophilus* exhibits distinct protective effects against arthritis, indicating that a combination of multiple strains may be necessary to effectively confer protection against RA.

A study conducted by researchers at New York University found that the human gut bacterium, *Prevotella copri*, may mediate the development of RA.[44,45] These researchers theorize that microbial and dietary metabolites, such as short- and medium-chain fatty acids, have immunomodulatory properties that could be harnessed to treat rheumatic diseases.[46] In our study, we measured the production of short-chain fatty acids (SCFAs) in response to a mixture of *L. acidophilus*. The primary SCFAs produced were acetic acid, propionic acid, and butyric acid. Notably, the levels of acetic acid, propionic acid, and butyric acid in the gut of CIA rats were significantly lower compared to those in the control group. However, when treated with mixed strains of *L. acidophilus*, the production of acetic acid and butyric acid by the intestinal microbiota of CIA rats increased significantly. Acetic acid is known to participate in cellular metabolic pathways, maintain intestinal integrity, and regulate lipid and carbohydrate metabolism.[47] Propionic acid has been shown to possess anti-inflammatory and antibacterial properties, which help protect the gut from pathogens, reduce liver cholesterol synthesis, and improve lipid metabolism.[48] As an energy source for colon cells, butyric acid regulates various intestinal functions, including immune regulation, intestinal development, cell differentiation, and gene expression, thereby reducing oxidative stress and inflammation.[49] SCFAs play a significant role in the prevention and treatment of various diseases, such as obesity,[50] cardiovascular diseases,[51] diabetes,[52] neuropathic diseases[53] and periodontal diseases.[54] These findings underscore the importance of SCFAs in inhibiting disease development and maintaining overall health. The mixed strains of *L. acidophilus* screened in this study may contribute to protection against RA by influencing the production of acetic acid and butyric acid.

In addition to SCFAs produced by the gut microbiota, the metabolites in blood were also affected by CIA modeling. The metabolites in blood of CIA rats were significantly different from those in normal rats. Among the top 10 differential metabolites, lipids and lipid molecules and organic acids and their derivatives account for the majority. Glycerophospholipids and organic acids and their derivatives were found in both upregulated and dow-regulated differential metabolites. The correlation analysis showed that *Akkermansia*, *Lachnospiraceae*_NK4A136_group, and *Ruminococcus* were correlated with these glycerophospholipids and organic acids and their derivatives. As a new generation of probiotics, *Akkermansia* has been widely studied. Metabolic disorders, including obesity, type 2 diabetes, non-alcoholic fatty liver disease and cardiovascular disease, are associated with the reduced abundance of *Akkermansia* spp.[55] *Lachnospiraceae* is a

family in the phylum *Firmicutes*, found mainly in the intestinal tract of humans and mammals. All members of this family are anaerobic bacteria that produce short-chain fatty acids, especially butyric acid, through fermentation metabolism, which is important for the prevention of colon cancer in humans.[56] *Ruminococcus* is "the key bacteria in degrading resistant starch", but is also associated with intestinal diseases (IBS, IBD, Crohn, *etc*.), immune diseases (allergies, eczema, asthma, *etc*.), and neurological diseases (autism, depression, *etc*.).[57] In this study, single strains of *L. acidophilus* did not affect blood metabolites in CIA rats. However, there have been reports of *Lactobacillus* affecting blood metabolites.[58,59]

5. Conclusion

In this study, mixed strains of *Lactobacillus acidophilus* were screened for their protective effects against collagen-induced arthritis. The results indicated that the mixed strains exerted their effects through multiple single-strain alleviations rather than relying on the impact of a single strain. Additionally, short-chain fatty acids, specifically acetic acid and butyric acid, may play a crucial role in providing protection against collagen-induced arthritis. This study offers valuable data to support the application of probiotics in the prevention of rheumatoid arthritis.

Author contributions

YY: writing – review & editing. QH: project administration, writing – review & editing. XZ: resources, supervision, writing – review & editing. ZL: funding acquisition, methodology, supervision, and writing – review & editing.

Data availability

All relevant data are within the article.

Conflicts of interest

The authors declare that they have no conflicts of interest for this work.

Acknowledgements

This work was supported by the Shanghai State-owned Assets Supervision and Administration Commission Enterprise Innovation Development and Capacity Enhancement Program (No. 2022013); the National Key R&D Program of China (2022YFD2100704). The authors are thankful to the State Key Laboratory of Dairy Biotechnology, Shanghai Engineering Research Center of Dairy Biotechnology, Bright Dairy & Food Co., Ltd, Shanghai, China, for providing the various resources for the completion of the current article.

References

1 J. S. Smolen, D. Aletaha, A. Barton, G. R. Burmester, P. Emery, G. S. Firestein, A. Kavanaugh, I. B. McInnes, D. H. Solomon, V. Strand and K. Yamamoto, Rheumatoid arthritis, *Nat. Rev. Dis. Primers*, 2018, **4**, 18001.
2 C. C. Rosenbaum, D. P. O'Mathúna, M. Chavez and K. Shields, Antioxidants and antiinflammatory dietary supplements for osteoarthritis and rheumatoid arthritis, *Altern. Ther. Health Med.*, 2010, **16**, 32–40.
3 S. Viatte and A. Barton, Genetics of rheumatoid arthritis susceptibility, severity, and treatment response, *Semin. Immunopathol.*, 2017, **39**, 395–408.
4 E. W. Karlson and K. Deane, Environmental and gene-environment interactions and risk of rheumatoid arthritis, *Rheum. Dis. Clin. North Am.*, 2012, **38**, 405–426.
5 A. I. Catrina, K. D. Deane and J. U. Scher, Gene, environment, microbiome and mucosal immune tolerance in rheumatoid arthritis, *Rheumatology*, 2016, **55**, 391–402.
6 J. U. Scher, V. Joshua, A. Artacho, S. Abdollahi-Roodsaz, J. Öckinger, S. Kullberg, M. Sköld, A. Eklund, J. Grunewald, J. C. Clemente, C. Ubeda, L. N. Segal and A. I. Catrina, The lung microbiota in early rheumatoid arthritis and autoimmunity, *Microbiome*, 2016, **4**, 60.
7 J. Chen, K. Wright, J. M. Davis, P. Jeraldo, E. V. Marietta, J. Murray, H. Nelson, E. L. Matteson and V. Taneja, An expansion of rare lineage intestinal microbes characterizes rheumatoid arthritis, *Genome Med.*, 2016, **8**, 43.
8 M. M. Nielen, D. van Schaardenburg, H. W. Reesink, R. J. van de Stadt, I. E. van der Horst-Bruinsma, M. H. de Koning, M. R. Habibuw, J. P. Vandenbroucke and B. A. Dijkmans, Specific autoantibodies precede the symptoms of rheumatoid arthritis: a study of serial measurements in blood donors, *Arthritis Rheum.*, 2004, **50**, 380–386.
9 S. Rantapää-Dahlqvist, B. A. W. de Jong, E. Berglin, G. Hallmans, G. Wadell, H. Stenlund, U. Sundin and W. J. van Venrooij, Antibodies against cyclic citrullinated peptide and IgA rheumatoid factor predict the development of rheumatoid arthritis, *Arthritis Rheumatol.*, 2003, **48**, 2741–2749.
10 D. S. Majka, K. D. Deane, L. A. Parrish, A. A. Lazar, A. E. Barón, C. W. Walker, M. V. Rubertone, W. R. Gilliland, J. M. Norris and V. M. Holers, Duration of preclinical rheumatoid arthritis-related autoantibody positivity increases in subjects with older age at time of disease diagnosis, *Ann. Rheum. Dis.*, 2008, **67**, 801–807.
11 E. W. Karlson, L. B. Chibnik, S. S. Tworoger, I. M. Lee, J. E. Buring, N. A. Shadick, J. E. Manson and K. H. Costenbader, Biomarkers of inflammation and development of rheumatoid arthritis in women from two prospective cohort studies, *Arthritis Rheum.*, 2009, **60**, 641–652.

12 J. Sokolove, R. Bromberg, K. D. Deane, L. J. Lahey, L. A. Derber, P. E. Chandra, J. D. Edison, W. R. Gilliland, R. J. Tibshirani, J. M. Norris, V. M. Holers and W. H. Robinson, Autoantibody epitope spreading in the pre-clinical phase predicts progression to rheumatoid arthritis, *PLoS One*, 2012, **7**, e35296.
13 V. M. Holers, M. K. Demoruelle, K. A. Kuhn, J. H. Buckner, W. H. Robinson, Y. Okamoto, J. M. Norris and K. D. Deane, Rheumatoid arthritis and the mucosal origins hypothesis: protection turns to destruction, *Nat. Rev. Rheumatol.*, 2018, **14**, 542–557.
14 R. Planas, R. Santos, P. Tomas-Ojer, C. Cruciani, A. Lutterotti, W. Faigle, N. Schaeren-Wiemers, C. Espejo, H. Eixarch, C. Pinilla, R. Martin and M. Sospedra, GDP-l-fucose synthase is a CD4(+) T cell-specific autoantigen in DRB3*02:02 patients with multiple sclerosis, *Sci. Transl. Med.*, 2018, **10**(462), eaat4301.
15 A. Pianta, S. L. Arvikar, K. Strle, E. E. Drouin, Q. Wang, C. E. Costello and A. C. Steere, Two rheumatoid arthritis-specific autoantigens correlate microbial immunity with autoimmune responses in joints, *J. Clin. Invest.*, 2017, **127**, 2946–2956.
16 N. Tai, J. Peng, F. Liu, E. Gulden and Y. Hu, Microbial antigen mimics activate diabetogenic CD8 T cells in NOD mice, *J. Exp. Med.*, 2016, **213**, 2129–2146.
17 Z. Fan, R. P. Ross, C. Stanton, B. Hou, J. Zhao, H. Zhang, B. Yang and W. Chen, Lactobacillus casei CCFM1074 Alleviates Collagen-Induced Arthritis in Rats via Balancing Treg/Th17 and Modulating the Metabolites and Gut Microbiota, *Front. Immunol.*, 2021, **12**, 680073.
18 S. Mörkl, M. I. Butler, A. Holl, J. F. Cryan and T. G. Dinan, Probiotics and the Microbiota-Gut-Brain Axis: Focus on Psychiatry, *Curr. Nutr. Rep.*, 2020, **9**, 171–182.
19 C. D'Mello, N. Ronaghan, R. Zaheer, M. Dicay, T. Le, W. K. MacNaughton, M. G. Surrette and M. G. Swain, Probiotics improve inflammation-associated sickness behavior by altering communication between the peripheral immune system and the brain, *J. Neurosci.*, 2015, **35**, 10821–10830.
20 X. Liu, B. Zeng, J. Zhang, W. Li, F. Mou, H. Wang, Q. Zou, B. Zhong, L. Wu, H. Wei and Y. Fang, Role of the Gut Microbiome in Modulating Arthritis Progression in Mice, *Sci. Rep.*, 2016, **6**, 30594.
21 D. D. Brand, K. A. Latham and E. F. Rosloniec, Collagen-induced arthritis, *Nat. Protoc.*, 2007, **2**, 1269–1275.
22 L. Wang, L. Hu, Q. Xu, T. Jiang, S. Fang, G. Wang, J. Zhao, H. Zhang and W. Chen, Bifidobacteria exert species-specific effects on constipation in BALB/c mice, *Food Funct.*, 2017, **8**, 3587–3600.
23 H. W. van Steenbergen, A. P. Cope and A. H. M. van der Helm-van Mil, Rheumatoid arthritis prevention in arthralgia: fantasy or reality?, *Nat. Rev. Rheumatol.*, 2023, **19**, 767–777.
24 L. Padyukov, Genetics of rheumatoid arthritis, *Semin. Immunopathol.*, 2022, **44**, 47–62.
25 K. Elsouri, V. Arboleda, S. Heiser, M. M. Kesselman and M. D. Beckler, Microbiome in Rheumatoid Arthritis and Celiac Disease: A Friend or Foe, *Cureus*, 2021, **13**, e15543.
26 J. S. Smolen and D. Aletaha, Rheumatoid arthritis therapy reappraisal: strategies, opportunities and challenges, *Nat. Rev. Rheumatol.*, 2015, **11**, 276–289.
27 M. M. Zaiss, H.-J. J. Wu, D. Mauro, G. Schett and F. Ciccia, The gut–joint axis in rheumatoid arthritis, *Nat. Rev. Rheumatol.*, 2021, **17**, 224–237.
28 S. B. Brusca, S. B. Abramson and J. U. Scher, Microbiome and mucosal inflammation as extra-articular triggers for rheumatoid arthritis and autoimmunity, *Curr. Opin. Rheumatol.*, 2014, **26**, 101–107.
29 A. Perez-Lopez, J. Behnsen, S.-P. Nuccio and M. Raffatellu, Mucosal immunity to pathogenic intestinal bacteria, *Nat. Rev. Immunol.*, 2016, **16**, 135–148.
30 J. Y. Yoo, M. Groer, S. V. O. Dutra, A. Sarkar and D. I. McSkimming, Gut Microbiota and Immune System Interactions, *Microorganisms*, 2020, **8**, 1587.
31 J. Wang, M. He, M. Yang and X. Ai, Gut microbiota as a key regulator of intestinal mucosal immunity, *Life Sci.*, 2024, **345**, 122612.
32 B. Bartok and G. S. Firestein, Fibroblast-like synoviocytes: key effector cells in rheumatoid arthritis, *Immunol. Rev.*, 2010, **233**, 233–255.
33 J. Chen, K. Wright, J. M. Davis, P. Jeraldo, E. V. Marietta, J. Murray, H. Nelson, E. L. Matteson and V. Taneja, An expansion of rare lineage intestinal microbes characterizes rheumatoid arthritis, *Genome Med.*, 2016, **8**, 43.
34 P. Liu, X.-y. Tan, H.-q. Zhang, K.-l. Su, E.-x. Shang, Q.-l. Xiao, S. Guo and J.-a. Duan, Optimal compatibility proportional screening of Trichosanthis Pericarpium - Trichosanthis Radix and its anti - Inflammatory components effect on experimental zebrafish and coughing mice, *J. Ethnopharmacol.*, 2024, **319**, 117096.
35 M. Marizzoni, P. Mirabelli, E. Mombelli, L. Coppola, C. Festari, N. Lopizzo, D. Luongo, M. Mazzelli, D. Naviglio, J.-L. Blouin, M. Abramowicz, M. Salvatore, M. Pievani, A. Cattaneo and G. B. Frisoni, A peripheral signature of Alzheimer's disease featuring microbiota-gut-brain axis markers, *Alzheimer's Res. Ther.*, 2023, **15**, 101.
36 S. Pavan, S. P. Gorthi, A. N. Prabhu, B. Das, A. Mutreja, K. Vasudevan, V. Shetty, T. Ramamurthy and M. Ballal, Dysbiosis of the Beneficial Gut Bacteria in Patients with Parkinson's Disease from India, *Ann. Indian Acad. Neurol.*, 2023, **26**, 908–916.
37 Z. Yan, L. Shi, J. Zhao, H. Zhang, G. Wang and W. Chen, Alleviating effects and mechanisms of Lactobacillus plantarum on muscle injury after high-intensity exercise in mice, *Food Ferment. Ind.*, 2024, **50**, 1–7.
38 X. Liu, Q. Zou, B. Zeng, Y. Fang and H. Wei, Analysis of Fecal Lactobacillus Community Structure in Patients with Early Rheumatoid Arthritis, *Curr. Microbiol.*, 2013, **67**, 170–176.
39 A. Picchianti-Diamanti, C. Panebianco, S. Salemi, M. L. Sorgi, R. Di Rosa, A. Tropea, M. Sgrulletti, G. Salerno, F. Terracciano, R. D'Amelio, B. Laganà and V. Pazienza, Analysis of Gut Microbiota in Rheumatoid Arthritis Patients: Disease-Related Dysbiosis and Modifications Induced by Etanercept, *Int. J. Mol. Sci.*, 2018, **19**, 2938.

40 T. Van de Wiele, J. T. Van Praet, M. Marzorati, M. B. Drennan and D. Elewaut, How the microbiota shapes rheumatic diseases, *Nat. Rev. Rheumatol.*, 2016, **12**, 398–411.

41 J.-S. So, H.-K. Kwon, C.-G. Lee, H.-J. Yi, J.-A. Park, S.-Y. Lim, K.-C. Hwang, Y. H. Jeon and S.-H. Im, Lactobacillus casei suppresses experimental arthritis by down-regulating T helper 1 effector functions, *Mol. Immunol.*, 2008, **45**, 2690–2699.

42 K. Hatakka, J. Martio, M. Korpela, M. Herranen, T. Poussa, T. Laasanen, M. Saxelin, H. Vapaatalo, E. Moilanen and R. Korpela, Effects of probiotic therapy on the activity and activation of mild rheumatoid arthritis – a pilot study, *Scand. J. Rheumatol.*, 2003, **32**, 211–215.

43 L. M. Pineda, S. F. Thompson, K. Summers, F. de Leon, J. Pope and G. Reid, A randomized, double-blinded, placebo-controlled pilot study of probiotics in active rheumatoid arthritis, *Med. Sci. Monit.*, 2011, **17**, Cr347–Cr354.

44 J. U. Scher, A. Sczesnak, R. S. Longman, N. Segata, C. Ubeda, C. Bielski, T. Rostron, V. Cerundolo, E. G. Pamer, S. B. Abramson, C. Huttenhower and D. R. Littman, Expansion of intestinal Prevotella copri correlates with enhanced susceptibility to arthritis, *eLife*, 2013, **2**, e01202.

45 J. U. Scher, C. Ubeda, M. Equinda, R. Khanin, Y. Buischi, A. Viale, L. Lipuma, M. Attur, M. H. Pillinger, G. Weissmann, D. R. Littman, E. G. Pamer, W. A. Bretz and S. B. Abramson, Periodontal disease and the oral microbiota in new-onset rheumatoid arthritis, *Arthritis Rheum.*, 2012, **64**, 3083–3094.

46 S. Abdollahi-Roodsaz, S. B. Abramson and J. U. Scher, The metabolic role of the gut microbiota in health and rheumatic disease: mechanisms and interventions, *Nat. Rev. Rheumatol.*, 2016, **12**, 446–455.

47 G. Merli, A. Becci, A. Amato and F. Beolchini, Acetic acid bioproduction: The technological innovation change, *Sci. Total Environ.*, 2021, **798**, 149292.

48 P. Markowiak-Kopeć and K. Śliżewska, The Effect of Probiotics on the Production of Short-Chain Fatty Acids by Human Intestinal Microbiome, *Nutrients*, 2020, **12**, 1107.

49 A. Bedford and J. J. A. N. Gong, Implications of butyrate and its derivatives for gut health and animal production, *Anim. Nutr.*, 2018, **4**, 151–159.

50 A. Jiao, B. Yu, J. He, J. Yu, P. Zheng, Y. Luo, J. Luo, H. Yan, Q. Wang, H. Wang, X. Mao and D. Chen, Sodium acetate, propionate, and butyrate reduce fat accumulation in mice via modulating appetite and relevant genes, *Nutrition*, 2021, **87–88**, 111198.

51 A. Haghikia, F. Zimmermann, P. Schumann, A. Jasina, J. Roessler, D. Schmidt, P. Heinze, J. Kaisler, V. Nageswaran, A. Aigner, U. Ceglarek, R. Cineus, A. N. Hegazy, E. P. C. van der Vorst, Y. Döring, C. M. Strauch, I. Nemet, V. Tremaroli, C. Dwibedi, N. Kränkel, D. M. Leistner, M. M. Heimesaat, S. Bereswill, G. Rauch, U. Seeland, O. Soehnlein, D. N. Müller, R. Gold, F. Bäckhed, S. L. Hazen, A. Haghikia and U. Landmesser, Propionate attenuates atherosclerosis by immune-dependent regulation of intestinal cholesterol metabolism, *Eur. Heart J.*, 2022, **43**, 518–533.

52 C. Dang, K. Zhao, H. Li, H. Zhu, X. Wang and S. Wang, Current studies on relationship between short-chain fatty acids and type 2diabetes mellitus, *Chin. J. Microecol.*, 2021, **33**, 1471–1475.

53 J. Liu, H. Li, T. Gong, W. Chen, S. Mao, Y. Kong, J. Yu and J. Sun, Anti-neuroinflammatory Effect of Short-Chain Fatty Acid Acetate against Alzheimer's Disease via Upregulating GPR41 and Inhibiting ERK/JNK/NF-κB, *J. Agric. Food Chem.*, 2020, **68**, 7152–7161.

54 A. D. Rudin, A. Khamzeh, V. Venkatakrishnan, A. Basic, K. Christenson and J. Bylund, Short chain fatty acids released by Fusobacterium nucleatum are neutrophil chemoattractants acting via free fatty acid receptor 2 (FFAR2), *Cell. Microbiol.*, 2021, **23**, e13348.

55 P. D. Cani, C. Depommier, M. Derrien, A. Everard and W. M. de Vos, Akkermansia muciniphila: paradigm for next-generation beneficial microorganisms, *Nat. Rev. Gastroenterol. Hepatol.*, 2022, **19**, 625–637.

56 R. Liu, C. Peng, D. Jing, Y. Xiao, W. Zhu, S. Zhao, J. Zhang, X. Chen and J. Li, Lachnospira is a signature of antihistamine efficacy in chronic spontaneous urticaria, *Exp. Dermatol.*, 2022, **31**, 242–247.

57 D. Pal and B. Mukhopadhyay, Chemical Synthesis of β-l-Rhamnose Containing the Pentasaccharide Repeating Unit of the O-Specific Polysaccharide from a Halophilic Bacterium Halomonas ventosae RU5S2EL in the Form of Its 2-Aminoethyl Glycoside, *J. Org. Chem.*, 2021, **86**, 8683–8694.

58 S. M. M. Pedersen, C. Nebel, N. C. Nielsen, H. J. Andersen, J. Olsson, M. Simrén, L. Öhman, U. Svensson, H. C. Bertram and A. Malmendal, A GC-MS-based metabonomic investigation of blood serum from irritable bowel syndrome patients undergoing intervention with acidified milk products, *Eur. Food Res. Technol.*, 2011, **233**, 1013–1021.

59 A. K. Naik, U. Pandey, R. Mukherjee, S. Mukhopadhyay, S. Chakraborty, A. Ghosh and P. Aich, Lactobacillus rhamnosus GG reverses mortality of neonatal mice against Salmonella challenge, *Toxicol. Res.*, 2019, **8**, 361–372.